






Systematic paleontology of macroalgal fossils from the Tonian Mackenzie Mountains Supergroup

Katie M. Maloney,^{1,2*}  Dakota P. Maverick,^{1,3} James D. Schiffbauer,^{3,4}  Galen P. Halverson,² 
Shuhai Xiao,⁵  and Marc Laflamme¹ 

¹Department of Chemical and Physical Sciences, University of Toronto Mississauga, Mississauga, ON L5L 1C6, Canada <katie.maloney@mail.utoronto.ca>, <mrhvyz@missouri.edu>, <marc.laflamme@utoronto.ca>

²Department of Earth and Planetary Sciences/GEOTOP, McGill University, Montréal, QC H3A 0E8, Canada <galen.halverson@mcgill.ca>

³Department of Geological Sciences, University of Missouri, Columbia, MO 65211, USA <schiffbauerj@missouri.edu>

⁴X-ray Microanalysis Core, University of Missouri, Columbia, MO 65211, USA

⁵Department of Geosciences, Virginia Tech, Blacksburg, VA 24061, USA <xiao@vt.edu>

Abstract.—Proterozoic eukaryotic macroalgae are difficult to interpret because morphological details required for proper phylogenetic studies are rarely preserved. This is especially true of morphologically simple organisms consisting of tubes, ribbons, or spheres that are commonly found in a wide array of bacteria, plants, and even animals. Previous reports of exceptionally preserved Tonian (ca. 950–900 Ma) fossils from the Dolores Creek Formation of Northwestern Canada feature enough morphological evidence to support a green macroalgal affinity. However, the affinities of two additional forms identified on the basis of the size distribution of available specimens remain undetermined, while the presence of three unique algal forms supports other reports of increasing algal diversity in the early Neoproterozoic. *Archaeochaeta guncho* new genus new species is described as a green macroalga on the basis of its well-preserved morphology consisting of an unbranching, uniseriate thallus with uniform width throughout and possessing an elliptical to globose anchoring holdfast. A larger size class of ribbon-like forms is interpreted as *Vendotaenia* sp. A third size class is significantly smaller than *Archaeochaeta* n. gen. and *Vendotaenia*, but in the absence of clear morphological characters, it remains difficult to assign. As *Archaeochaeta* n. gen. and *Vendotaenia* represent photoautotrophic taxa, these findings support the hypothesis of increasing morphological complexity and phyletic diversification of macroalgae during the Tonian, leading to dramatic changes within benthic marine ecosystems before the evolution of animals.

Introduction

The early Neoproterozoic Mackenzie Mountains Supergroup in northwest Canada hosts exceptionally preserved macrofossils interpreted to represent multicellular eukaryotes, including probable macroalgae (Hofmann and Aitken, 1979; Hofmann, 1985; Maloney et al., 2021, 2022). During the Neoproterozoic Era (1000–539 Ma), eukaryotic algae evolved and proliferated through marine ecosystems, becoming the dominant primary producers by at least the Cryogenian (~720–635 Ma; Brocks et al., 2017; Sánchez-Baracaldo et al., 2017; Isson et al., 2018). This algal diversification is interpreted to represent a major step-wise change in the makeup of Neoproterozoic paleoenvironments by restructuring benthic habitats and biogeochemical cycles (Del Cortona et al., 2020), which are thought to have played an important role in setting the stage for the emergence of diverse animals (Brocks, 2018).

To understand the drivers of the critical change in Earth's biosphere, it is important to examine and document fossil algal diversity (LoDuca et al., 2017). However, the current

record from the Proterozoic is limited due to taphonomic biases associated with the fossilization of soft tissues (Muscente et al., 2017; Maloney et al., 2022). Recently, calls for detailed investigations of the fossil record during poorly documented time intervals (Cohen and Macdonald, 2015; Bykova et al., 2020) have highlighted the sparse records of the Tonian (e.g., Pang et al., 2018; Xiao and Tang, 2018) and Cryogenian (e.g., Ye et al., 2015) periods. These intervals are of particular interest because Proterozoic macroalgae experienced a significant morphological diversification during this time (Xiao and Tang, 2018; Bykova et al., 2020; Tang et al., 2020).

The extensive Proterozoic stratigraphy in Arctic Canada provides an ideal locality to target Tonian eukaryotic fossils. Previous studies have yielded numerous exceptional fossil localities (Hofmann and Aitken, 1979; Butterfield, 2000; Cohen and Macdonald, 2015; Loron et al., 2019), which include poorly constrained forms such as the Little Dal macrobiota (Hofmann and Aitken, 1979; Hofmann, 1985) and the Rusty and Wynniatt assemblages (Butterfield, 2005a, b); vase-shaped (Strauss et al., 2014; Cohen et al., 2017a) and scale-like (Cohen and Knoll, 2012) microfossils from the Fifteenmile Group; Shaler Supergroup fungal microfossils (Loron et al., 2019); red algal microfossils of the Bylot basins (Butterfield, 1990; Knoll et al., 2013;

*Corresponding author.

Gibson et al., 2018); and purported sponge fossils from the Little Dal Group (Turner, 2021).

Recent studies of the Dolores Creek Formation, the basal unit of the Tonian Mackenzie Mountains Supergroup, have yielded 300+ fossils representing three distinct size classes (Maloney et al., 2021) that have yet to be formally described. Here we provide a detailed formal description of three new fossils from the Dolores Creek Formation, including a new species, *Archaeochaeta guncho* new genus new species, and likely examples of the oldest known *Vendotaenia* sp. We also discuss distinctive morphological characteristics that can be used to aid in identifying Proterozoic macroalgae, compare the morphology of the new fossils with other known Proterozoic life, and consider the consequences of these morphological advancements on Neoproterozoic ecosystems.

Geologic setting

The fossil-bearing beds of the Dolores Creek Formation outcrop at the headwaters of Hematite Creek River, a tributary of the Bonnet Plume River in the Wernecke Mountains near the Yukon–Northwest Territories (NWT) border in northwestern Canada (Fig. 1). The 950–900 Ma Dolores Creek Formation is the oldest of three formations in the Hematite Creek Group, which in turn is the oldest group in the Tonian Mackenzie Mountains Supergroup (950–775 Ma). Broadly equivalent Tonian strata across Arctic Canada include the Fifteenmile Group in western Yukon (Halverson et al., 2012; Macdonald et al., 2012) and the Shaler Supergroup in northern NWT (Rainbird et al., 1996). In the Wernecke Mountains, the Dolores Creek Formation unconformably overlies the Mesoproterozoic Pinguicula Group, which is a mixed siliciclastic and carbonate succession with a maximum age of 1380 Ma (Medig et al., 2010, 2012). The Black Canyon Creek Formation conformably overlies the Dolores Creek Formation and represents the shallowing-upward transition into tidally influenced deposits characterized by meter-scale carbonate–shale cycles (Turner, 2011).

The strata of the Dolores Creek Formation consist of fine-grained siliciclastic rocks (shale to siltstone) interbedded with microbial dolostone interpreted as marginal marine to offshore deposits (Turner, 2011; Maloney et al., 2021). The type section of the Dolores Creek Formation characteristically comprises ~300 m of strata but reaches a thicknesses of ~1,000 m in the southernmost studied sections, where it is informally divided into a lower and upper unit that together represent a single regressive sequence (Gibson et al., 2019). The lower unit comprises ~600 m of predominantly shales and siltstones with interbedded interclast breccias and wackestones interpreted as gravity-flow deposits (“debrites”). Increasing carbonate content within the debrites, and the occurrence of stromatolitic olistoliths up-section, hint at progradation of a shelf margin and passage the overlying unit, which consists of biostromes of columnar stromatolites interbedded with organic-rich shales. The strata within the lower Dolores Creek Formation where the fossils abruptly appear are interpreted as shelf-margin deposits controlled by a fault escarpment that formed in response to an extensional episode during the formation of the Hematite Creek Basin (Turner, 2011; Gibson et al., 2019).

The first in situ carbonate unit from the Dolores Creek Formation is a minor microbially laminated bed ~50 m below the fossil beds, while the first semi-continuous stromatolitic biostromes occur ~20 m above the fossil interval (Fig. 1). The fossils occur within gravity-flow deposits that record the downslope movement and deposition of sediment from the photic zone at the platform margin (Maloney et al., 2021). The fossils appear along bedding planes throughout slabs interpreted to record rapid burial events on the basis of the organization of the thin beds of differing grain sizes interbedded with floatstone (carbonate debrites). These depositional processes contributed to the exceptional preservation of these organisms by emplacing them within (presumably) anoxic, sulfate-reducing conditions (Cai et al., 2012; Schiffbauer et al., 2014; Maloney et al., 2022).

Materials and methods

More than 340 individual fossil specimens from 17 in situ slabs collected from six distinct horizons, and five slabs with exceptionally preserved fossils recovered from float, were investigated (Figs. 1–5). Slabs contain 3–40 total specimens, with 1–22 per bedding surface. Some slabs were susceptible to fracturing, which exposed additional bedding surfaces that contained fossils. Such surfaces were included during data collection. In slabs with a high density of overlapping specimens, individual fossils were at times difficult to discern and in turn were excluded from both the total specimen count and the length measurements. Specimens were observed under a stereoscope. Whenever possible, morphometric data—including total organism length, cell height and width, cell-wall thickness, differentiated cells, specimen features (true and false branching, twisting/deformation, overlapping, tapering ends), and specimen shape (straight, slightly curved, U-shaped, V-shaped, J-shaped, or S-shaped)—were collected using the open-source program ImageJ (Schneider et al., 2012). Three distinct size classes of fossils were defined on the basis of widths (Fig. 6). The widest specimens ($n = 19$, width = 1.0–1.7 mm) are interpreted to represent *Vendotaenia* sp. The medium-sized specimens ($n = 304$, width = 0.20–0.85 mm) show significant morphological detail and are attributed to a newly defined form, *Archaeochaeta guncho* n. gen. n. sp. Specimens of the narrowest size class ($n = 90$, width = 0.03–0.06 mm) were abundant throughout the section and found on every slab collected, although their small size and lack of detail precludes any definitive taxonomic identification and phylogenetic interpretation.

Selected specimens of the two smallest size classes ($n = 12$) were targeted for additional analyses using scanning electron microscopy (SEM) with energy dispersive X-ray spectroscopy (EDS) and tomographic X-ray microscopy (μ CT) at the University of Missouri X-ray Microanalysis Core Laboratory (see Maloney et al., 2022). A Zeiss Sigma 500 variable-pressure system equipped with dual, co-planar Bruker XFlash spectrometers was used to conduct the SEM and EDS analyses at identical beam and chamber conditions (20 keV beam accelerating voltage, 40 nA high current mode, 60 μ m aperture, and 20 Pa chamber pressure with a 99.999% nitrogen atmosphere). Z-contrast imaging was conducted using a high-definition five-segment backscatter detector, and a cascade current detector was used

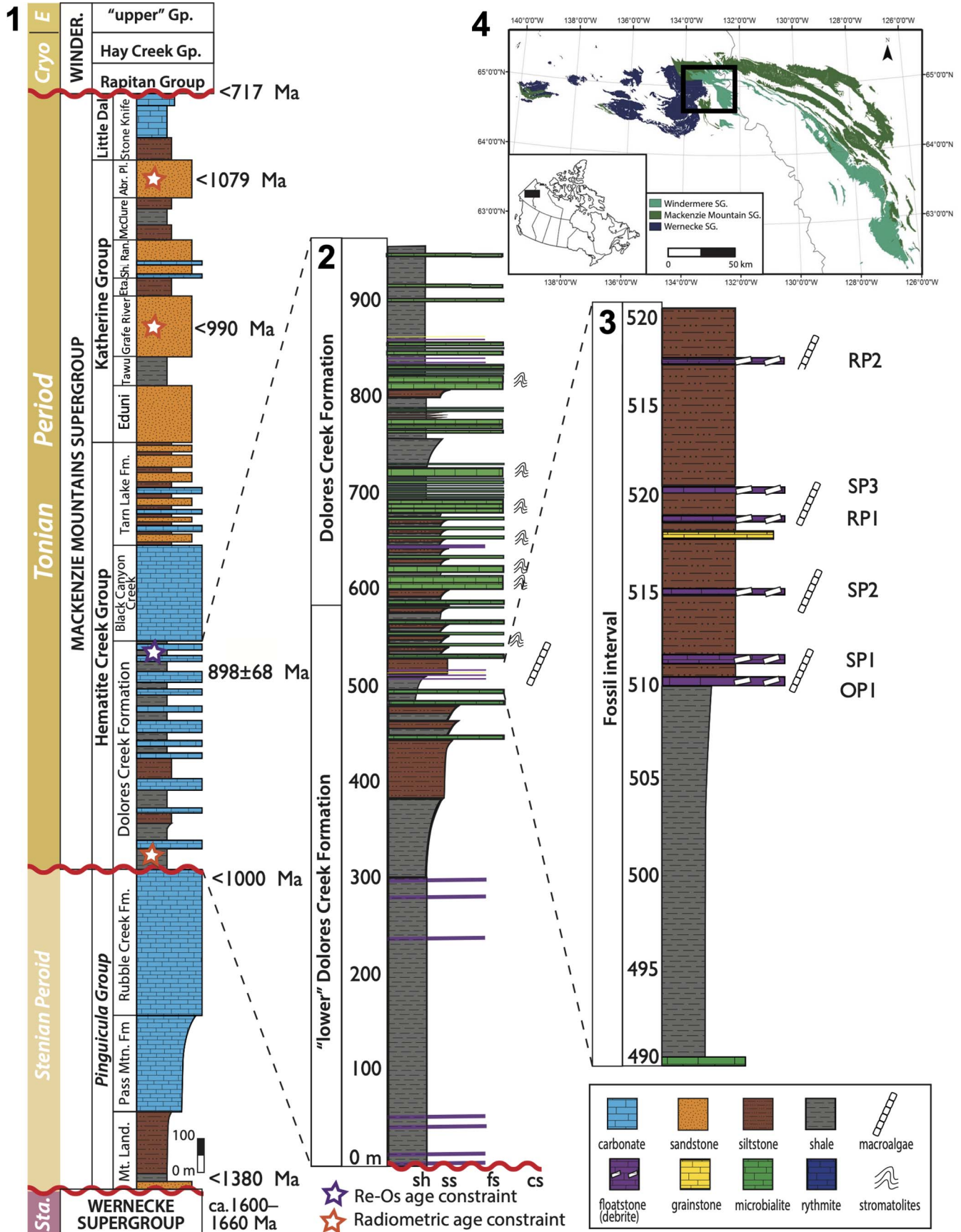


Figure 1. Fossil locality. (1) Stratigraphy log of the Mackenzie Mountains Supergroup with radiometric (purple and orange star) and stratigraphic age constraints. (2) Measured section where fossils were recovered (Yukon, Canada, 64°41'17.6"N; 133°14'30.3"W), scale in meters. (3) Fossil interval enlarged with individual fossil horizons labeled (OP1, SP1, SP2, RP1, SP3, RP2), scale in meters; x axis shows relative grain sizes from mud/shale to coarse sand. (4) Map of the Proterozoic inliers, including the Wernecke, Mackenzie Mountains, and Windermere supergroups that span the Yukon and Northwest Territories border in northwestern Canada, with a black rectangle indicating the study area. Gp. = Group; Fm. = Formation; Sta. = Statherian Period; Eta = Etagogchile Formation; Sh. Ran. = Shatter Ridge Formation; Abr. Pl. = Abraham Plains Formation; Cryo = Cryogenian Period; E = Ediacaran Period; Winder. = Windermere supergroup; Mt. Land. = Mount Landreville Formation; Pass Mtn. = Pass Mountain Formation; SG = supergroup.

for secondary electron imaging in low vacuum. EDS elemental mapping was used to characterize the composition of the specimens, with both spectrometers used in tandem (360 seconds live time, 120 µm aperture). A single specimen preserved in three dimensions was further analyzed through µCT (Zeiss Xradia 510 Versa). The operating conditions were as follows: 80 kV source voltage, 7 W source power, LE3 (low energy) filter, 0.4x objective, 4.5 sec exposure, 2001 projections at 360°, and voxel size 11.09 µm.

Repository and institutional abbreviation.—Types, figured, and other specimens are deposited with the Royal Ontario Museum (ROMIP) in Toronto, Canada (ROMIP66160–ROMIP66170; ROMIP66282–ROMIP66292).

Systematic paleontology

The size distribution of the fossil assemblage was investigated to determine whether these fossils include distinct species. When fossil widths are compared, three distinct size classes emerge (Fig. 6) regardless of preservational quality (see Supplemental Data 1). Although the affinities of many Proterozoic fossils remain controversial, a subset of exceptional Dolores Creek Formation fossils have clear morphological characteristics that aid in their interpretation as eukaryotic macroalgae with a possible green algal affinity (Maloney et al., 2021); thus, the International Code of Nomenclature for Algae, Fungi, and Plants (Turland et al., 2018) is followed in this paper. The largest size class ranges from 1.0 to 1.7 mm, and its specimens are attributed to *Vendotaenia* Gnilovskaya, 1971 on the basis of their ribbon-like morphology and comparable size. The middle size class has the most complex morphology preserved, with holdfasts, longitudinal striations, and large cells with a thallus width ranging from 0.20 to 0.85 mm. The smaller fossils range in width from 0.03 to 0.06 mm and show dichotomous branching. Given that these smaller fossils lack any morphologically distinct characters, we have not assigned them to a specific taxonomic rank and instead provide a description of the fossils as well as comparisons with other Proterozoic fossils.

Kingdom Archaeplastida Adl et al., 2005
Phylum Viridiplantae Cavalier-Smith, 1981
Division Chlorophyta Reichenbach, 1828
Genus *Archaeochaeta* new genus

Type species.—*Archaeochaeta guncho* n. gen. n. sp. by monotypy.

Diagnosis.—As per species.

Occurrence.—Dolores Creek Formation, Mackenzie Mountains Supergroup, near the headwaters of Hematite Creek (64°

41'17.6"N; 133°14'30.3"W), Wernecke Mountains, Yukon Territory, Canada; Tonian (Maloney et al., 2021).

Etymology.—From Greek, *archaeo*, meaning “ancient,” with reference to the geological age of this genus, and *chaeto*, meaning “hair or bristle,” owing to its morphological comparison to the extant green algal genus *Chaetomorpha* Kützinger, 1845.

Remarks.—As per species.

Archaeochaeta guncho new species
Figures 2, 3, 4.3, 5.5, 5.7

Holotype.—Specimen 59.18 on ROMIP66169, illustrated in Figure 2.2, 2.3.

Paratype.—Specimen 59.28 on ROMIP6616, illustrated in Figure 2.1, 2.5.

Diagnosis.—Multicellular, uniseriate, unbranching thallus of uniform width. Individual cells are rectangular (width greater than length) with two (double) septa between adjacent cells and rib-like cell-wall ornamentation parallel to the thallus length. Ellipsoidal to globose holdfasts rarely present.

Occurrence.—Dolores Creek Formation, Mackenzie Mountains Supergroup, near the headwaters of Hematite Creek, Wernecke Mountains, Yukon Territory, Canada; Tonian (Maloney et al., 2021).

Description.—Uniseriate filament of multiple individual cells. Thallus length ranges from 1.0 to 32.7 mm (n = 304 specimens on 20 fossil slabs) with sharp terminations at one or both ends of the filaments. Thallus widths are consistent along the entire length, with an average width of 0.67 mm (ranges from 0.27 to 0.80 mm, n = 304). Each well-preserved cell contains a recalcitrant cell wall with rib-like cell-wall ornamentation (Figs. 2.3–2.7, 3) resembling longitudinal striations in modern green algae (Gontcharov and Watanabe, 1999; Maloney et al., 2021).

Each filament is composed of cells with transverse cell walls or septa (perpendicular to thallus length) preferentially preserved compared with the lateral cell walls (parallel to thallus length; Fig. 2.3–2.7). Lateral cell walls are on average 0.06 mm thick (n = 40) while transverse cell walls are 0.10 mm thick (n = 410). Individual cells are rectangular (presumably originally cylindrical), ranging from 0.2 to 1.0 mm long and 0.3 to 0.7 mm wide. The presence of double septa rather than a single thick transverse cell wall is suggested by the occurrence of a clear gap between two adjacent cells (Fig. 2.3–2.7). Holdfasts are rare, but when found they are elliptical to globose and are located at the terminus of the thallus (Fig. 2.1–2.3, 2.5, 2.7). Holdfasts range from 0.19 to

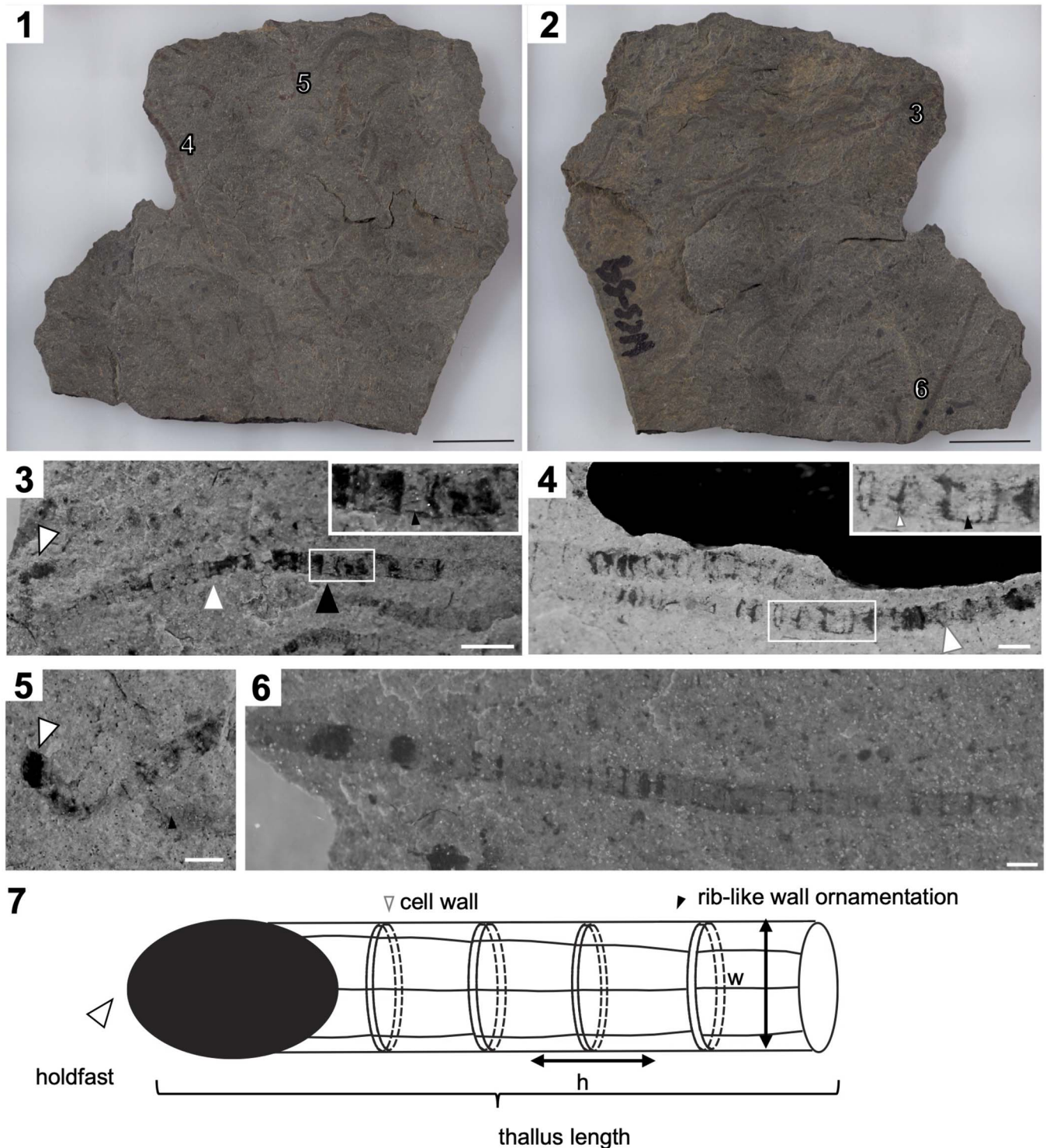


Figure 2. *Archaeochaeta guncho* n. gen. n. sp. (1, 2) ROMIP66169 fossil slab showing the distribution of macroalgal fossils on each side and the locations of enlarged specimens in (3–6). (3) Holotype specimen 59.18 with an elongated holdfast (white arrowhead with black outline), longitudinal striations (black arrowhead, inset), and double septa (white arrowhead with gray outline). (4) Specimen 59.22, longitudinal striations (black arrowhead, inset) and double septa (white arrowhead with gray outline, inset). (5) Paratype specimen 59.28, elongated holdfast (white arrowhead with black outline) and longitudinal striations (black arrowhead). (6) Specimen 59.9 with individual cells. (7) Idealized sketch showing morphological traits and morphometric measurements. Scale bars = 1 mm.

0.98 mm (mean = 0.53 mm, $n = 6$) in the longest dimension and from 0.19 to 0.58 mm (mean = 0.40 mm, $n = 6$) in the shortest dimension. However, these unequal dimensions could represent a preservational bias of an originally spherical structure.

Etymology.—The fossils reported herein were recovered from the traditional territory of the First Nation of Na-Cho Nyak Dun. The species epithet *guncho* is derived from Northern Tutchone, the language of the First Nation of Na-Cho Nyak

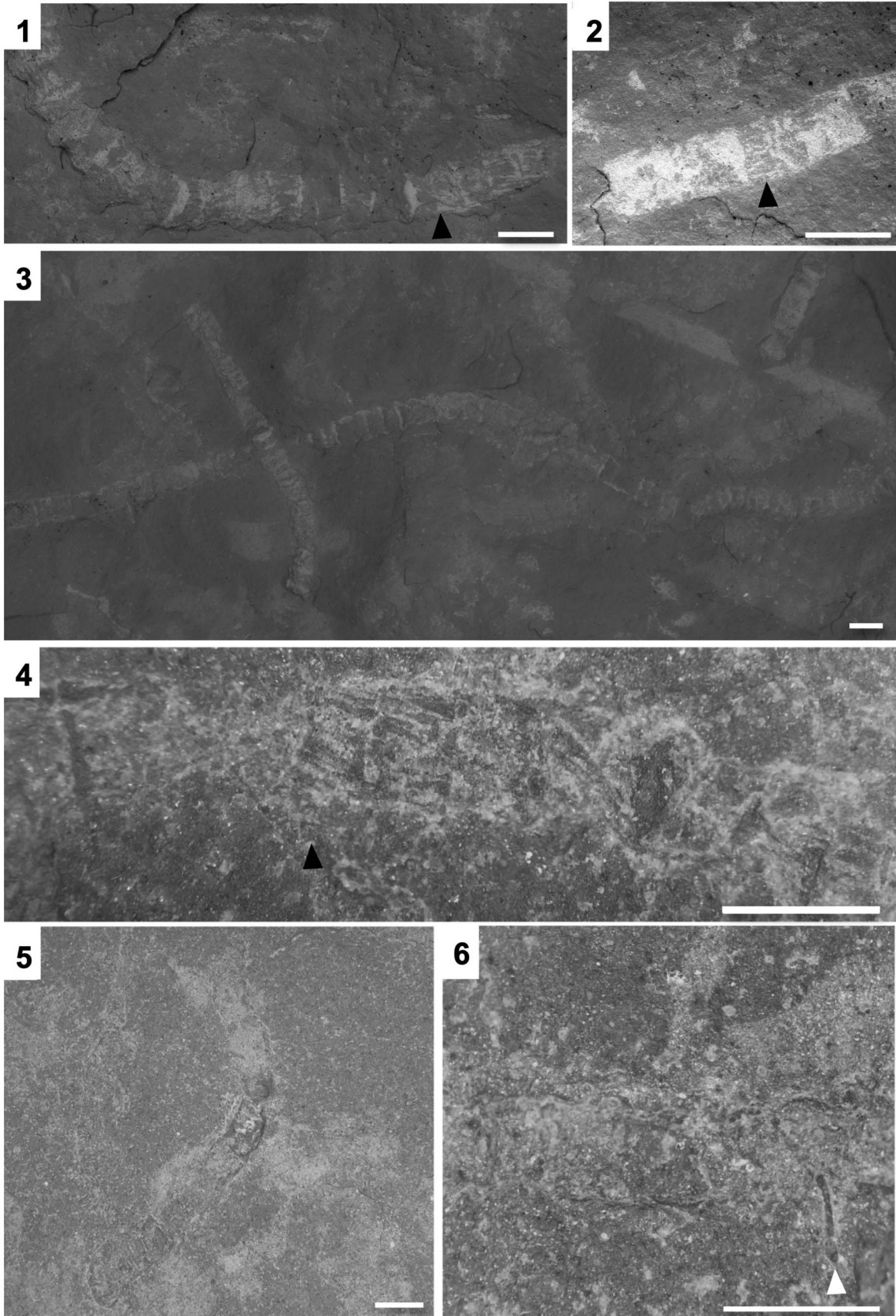




Figure 3. Three-dimensional (3D) preservation in *Archaeochaeta guncho* n. gen. n. sp. (1) ROMIP66170, 3D preservation of longitudinal striations (black arrowhead) in SEM image. (2) ROMIP66169, 2D preservation of longitudinal striations (black arrowhead) in SEM image. (3) ROMIP66170, 3D preservation of several fossils in SEM image. (4–6) Light microscope photos showing 3D preservation of ROMIP66170, showing fossil borders (dotted lines), longitudinal striations (black arrowhead), and a thin filament of unnamed species (white arrowhead). Scale bars = 1 mm.

Dun (Billy and Wheeler, 1998; Ritter, 2015), meaning “big worm.” The name references the large size and visible segment-like morphology of the organism.

Materials.—A total of 304 specimens from the Dolores Creek Formation, Mackenzie Mountains Supergroup, near the headwaters of Hematite Creek, Wernecke Mountains, Yukon Territory, Canada; Tonian (Maloney et al., 2021).

Remarks.—Specimens are fragmented (likely transported downslope via gravity flows; Maloney et al., 2021), and therefore the measured lengths best represent minimum estimates. The thallus is unbranching, with consistent width along its entire length. However, the preservational quality differs between transverse and lateral cell walls. The transverse cell walls (between cells) are generally 1.7 times the thickness of lateral cell walls (parallel to thallus length), which likely represents a taphonomic artifact created by the higher preservation potential of transverse double septa compared with cell walls.

Thallus architecture is important for higher-level classification. When specimens are found in dense accumulations and preserved as two-dimensional compressions (Maloney et al., 2022), it can be difficult to differentiate confidently between a single branching specimen and the overlap of two unbranching specimens of similar size (e.g., Fig. 2.4). We note that the thallus filaments have sharp terminations where they interact with another filament and that double septa are poorly preserved or even at times abruptly absent at the junction. We note that there is no cellular differentiation at the thallus junction or even any curvature change in the taphonomic “branching” angle. These features all point to a structurally simple uniserial unbranching thallus for *Archaeochaeta*.

Uniseriate filaments are common among green algae (South and Whittick, 1987), whereas the majority of modern brown algae possess parenchymatous cells, and red algae possess pseudoparenchymatous forms (Graham and Wilcox, 2000). Cells in parenchymatous thalli divide in all directions, resulting in a three-dimensional algal construction rather than a one-dimensional filamentous structure (Barsanti and Gualtieri, 2014). By contrast, pseudoparenchymatous forms are tessellations of multiple filaments that are intertwined and/or branched, preserving the filamentous construction (Barsanti and Gualtieri, 2014). Some modern rhodophytes, such as comsopogonophycans and bangiophycans (Yoon et al., 2016), possess a uniseriate filamentous construction in their thalli, but their filaments typically consist of uniquely arranged paired cells with multiseriate or corticated thalli (Krishnamurthy, 1962; Butterfield, 2000). Given that *A. guncho* n. gen. n. sp. consists of a uniseriate, filamentous thalli with unidirectional growth, it is unlikely that it represents a red or brown alga; the large size, uniseriate filamentous construction with elongated holdfasts, and rib-like wall ornamentation all support a green macroalgal affinity (Maloney et al., 2021).

The comparatively large size of *Archaeochaeta* invites comparison to the Proterozoic macrofossil *Grypania* Walter et al., 1976. However, *Archaeochaeta* has exceptionally preserved complex morphology with differentiated cell walls and holdfasts, while *Grypania* typically lacks such structures, although Sharma and Shukla (2009) have interpreted transverse markings as cell walls in specimens from India. Furthermore, *Grypania* is typically observed as coils whereas *Archaeochaeta* specimens are typically straight and only rarely curved, twisted, or folded over upon themselves, suggesting that the filaments had some degree of structural integrity or rigidity.

Eosolena Hermann in Hermann and Timofeev, 1985 from the late Mesoproterozoic Lakhanda biota (German and Podkovyrov, 2009; Hermann and Podkovyrov, 2014) and the Mesoproterozoic Kotuikan biota (Vorob’eva et al., 2015) can be compared to *Archaeochaeta* given their shared filamentous construction with a holdfast (German and Podkovyrov, 2009). However, *Eosolena* is notably smaller (<0.25 mm wide versus 0.27–0.80 mm; Vorob’eva et al., 2015). *Archaeochaeta* is also superficially similar to *Segmentothalpus asperus* Hermann in Yankauskas et al., 1989 from the ca. 1000 Ma Lakhanda biota, but the latter too is much narrower (~30 μm; German and Podkovyrov, 2009). The Mesoproterozoic–Tonian Lakhanda Group also includes “eosolenides tubular fossils,” an informal group of macroscopic organic-walled tubes that are slightly larger (0.4–1.0 mm) than the Dolores Creek macroalgae. Some eosolenides even have thin, straight, closely spaced fine fibro-lamellar striations, which are broadly comparable to the longitudinal striations observed within the cells of *Archaeochaeta*. Eosolenides segments are separated by membranes and vary from box-like (0.15–0.20 mm) to barrel-shaped (0.40–0.60 mm), the latter of which are similar in size to *Archaeochaeta*. However, the *Archaeochaeta* cells are wider than they are long whereas eosolenides segments are longer than they are wide.

The modern cyanobacterium *Nostoc flagelliforme* Harvey ex Molinari-Novoa et al. in Calvo-Pérez et al., 2016 (fat choy) is superficially similar to *Archaeochaeta* in that the colony of trichomes can reach up to 1 mm in diameter. However, the majority of the cells in *N. flagelliforme* are two orders of magnitude smaller (0.004–0.005 mm) than the cells within *Archaeochaeta* (Wang and Gu, 1984). In addition, *N. flagelliforme* hosts larger cells (heterocysts) that typically occur throughout the thallus (Gao, 1998), as opposed to the uniform cell size (except for the holdfast) of *Archaeochaeta*.

Genus *Vendotaenia* Gnilovskaya, 1971

Type species.—*Vendotaenia antiqua* Gnilovskaya 1971, p. 375.

Vendotaenia sp.
Figure 4.1–4.3

Occurrence.—Dolores Creek Formation, Mackenzie Mountains Supergroup, near the headwaters of Hematite Creek, Wernecke Mountains, Yukon Territory, Canada; Tonian.

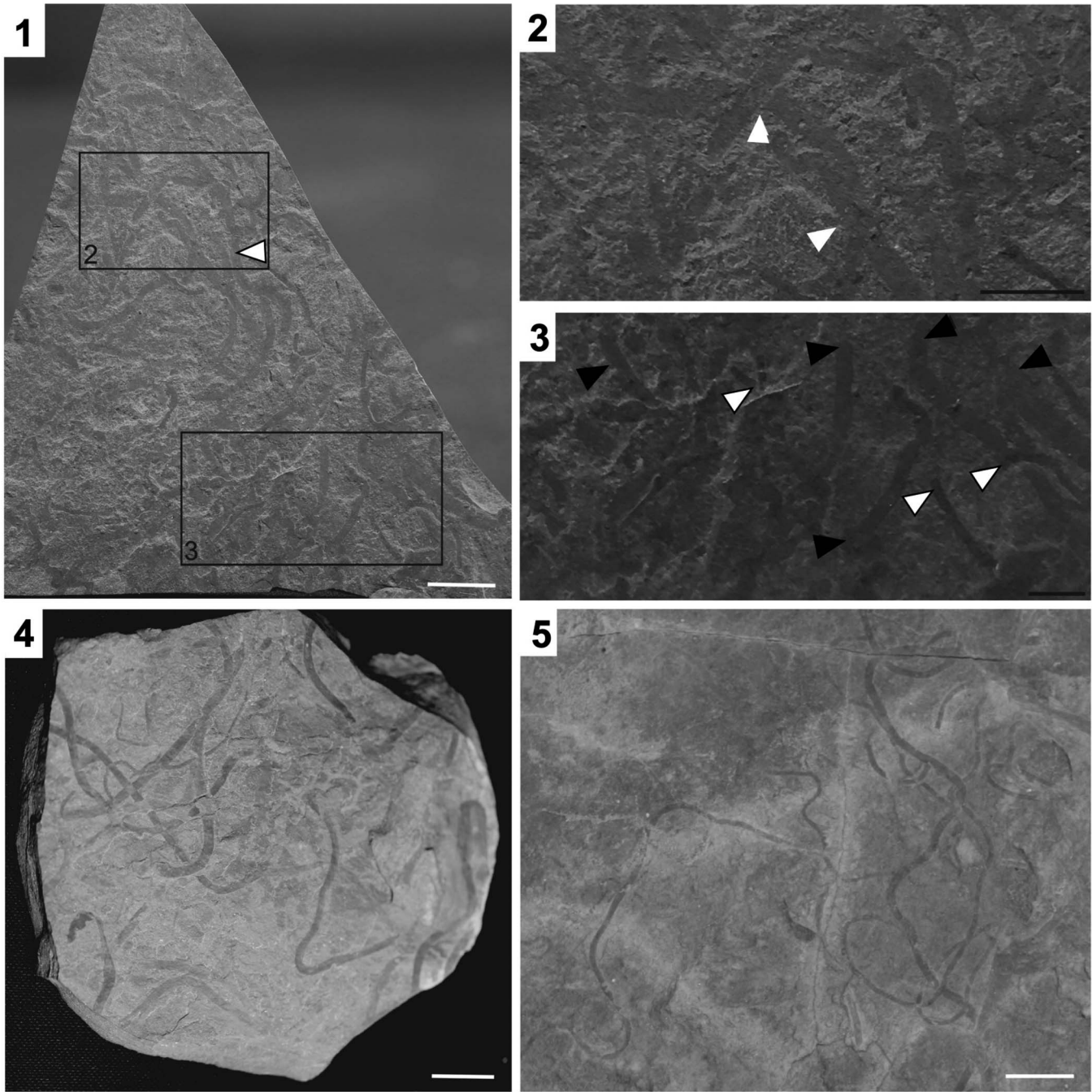


Figure 4. *Vendotaenia* sp. (1) Fossil slab ROMIP66283 with larger fossils assigned to *Vendotaenia* sp. (example indicated with white arrowhead) while smaller fossils are *Archaeochaeta guncho* n. gen. n. sp. (2) *Vendotaenia* sp. (labeled rectangle in (1)) showing overlapping specimens (white arrowheads). (3) *Archaeochaeta guncho* n. gen. n. sp. (white arrowhead with black outline) and *Vendotaenia* sp. (black arrowhead) in area marked by labeled rectangle in (1), demonstrating size difference between the two taxa. (4, 5) *Vendotaenia* sp. from the Ediacaran Feldschuhhorn Member of the Nama Group, Namibia, for morphological comparison. (1, 4, 5) White scale bars = 1 cm; (2, 3) black scale bars = 0.5 mm.

Description.—Specimens consist of a slender, ribbon-shaped thalli. Width: 1.01–1.69 mm; length: 4.96–40.8 mm ($n = 19$), with no variation along the length of the organism. Specimen length terminates sharply, and given the high density of specimens, numerous examples of overlap between specimens is noted (Fig. 4). Surficial features and cross-walls not evident.

Materials.—Nineteen specimens from the Dolores Creek Formation, Mackenzie Mountains Supergroup, near the

headwaters of Hematite Creek, Wernecke Mountains, Yukon Territory, Canada; Tonian.

Remarks.—One fossil slab with 28 specimens (nine specimens of *Archaeochaeta* and 19 of *Vendotaenia* sp.; Fig. 4.1–4.3) was recovered. *Vendotaenia* sp. differs from *Archaeochaeta* in its much larger overall size and complete absence of morphological characters on the fossil surface, such as striations or cell walls. *V. antiqua* typically includes visible

longitudinal striations (Gnilovskaya, 1971, 1990), which are missing from our specimens, although this absence could be taphonomic. For example, Gaucher et al. (2003, 2008) and Becker-Kerber et al. (2021) suggest that the longitudinal striations in *Vendotaenia* could result from the compression of an originally circular tube and caution with the use of this character for diagnostic purposes.

Vendotaenia sp. closely resembles tubular compression from the Vingerbreek and Felschuhhorn members of the Ediacaran Nama Group of Namibia (Fig. 4.4, 4.5). Cohen et al. (2009) assigned the Felschuhhorn specimens to *Vendotaenia antiqua* due to their sinuous bending, fine longitudinal striations, and rare branching (Gnilovskaya, 1971; Germs et al., 1986; Cohen et al., 2009). *Vendotaenia* sp. does superficially resemble the unassigned Vingerbreek population, falling within the size range of the Vingerbreek specimens (1.0–1.7 mm compared with 0.6–2.1 mm).

The morphology of *Vendotaenia* sp. warrants comparison with another filamentous fossil from the Mackenzie Mountains Supergroup, *Deltaenia mackenziensis* Hofmann, 1985, which shares a similar size range (width 0.3–1.5 mm) and a similar preservation mode with *Vendotaenia* sp. (both preserved as carbonaceous or pyritized compressions). However, *D. mackenziensis* exhibits clear branching and lacks the bending and twisting apparent in *Vendotaenia* sp., suggesting a greater structural rigidity (Hofmann, 1985). However, *Vendotaenia* sp. appears to be more rigid than *Grypania* from the Belt Supergroup, Montana (Walter et al., 1976; Han and Runnegar, 1992) since *Vendotaenia* sp. lacks any coiling. *Vendotaenia* sp. can also be compared to *Proterotainia* Walter et al., 1976, which shares a ribbon-like shape ranging from 0.6 to 2.0 mm wide and for which longitudinal striations are common (Walter et al., 1976). *Proterotainia* is much longer (up to 125 mm) than *Vendotaenia* sp., but the fragmentary nature of all specimens from northwestern Canada makes it difficult to compare them on the basis of length (Walter et al., 1976).

The phylogenetic affinity of *Vendotaenia* remains unresolved, and the taxon is poorly defined (Bykova et al., 2020). This genus was first interpreted as macroalgae (Gnilovskaya, 1983) on the basis of its morphological characteristics, including oogonia (the female sex organ of some algae and fungi) and cell walls (Cohen et al., 2009). The characteristic longitudinal striations in *Vendotaenia* are present in modern bacteria such as *Thioploca* Lauterborn, 1907 (Vidal, 1989), which tends to be an order of magnitude smaller (Cohen et al., 2009), and could instead represent the effects of compressing a three-dimensional tube into a two-dimensional film (Gaucher et al., 2003, 2008; Becker-Kerber et al., 2021). An algal interpretation for *Vendotaenia* remains probable given that the brown alga *Chorda* Stackhouse, 1797, the green alga *Enteromorpha* Link, 1820, and the red alga *Nemalion* Duby, 1830 all represent potential modern analogs (Cohen et al., 2009).

Despite previous interpretations of *Vendotaenia* as a brown alga (Phaeophyceae; Gnilovskaya, 1983), we follow Cohen et al. (2009), who proposed a green or red algal affinity as more likely, particularly considering that molecular clocks indicate a significantly younger (i.e., Mesozoic) origin for brown algae (Silberfeld et al., 2010; Bringle et al., 2020). By contrast, photosynthesizing eukaryotes, including red and green algal

lineages, are hypothesized to have originated in the mid-Proterozoic, with the diversification of major clades of Archaeplastida in the Neoproterozoic (Eme et al., 2014; Knoll, 2014; Yang et al., 2016; Hou et al., 2022). Notwithstanding limitations on interpretations imposed by taphonomy (Maloney et al., 2022), a green algal affinity for *Vendotaenia* is consistent with its overall large thallus size and longitudinal striations. Body fossils of both red (Butterfield, 2000; Gibson et al., 2018) and green (Tang et al., 2020) algae have been found in ca. 1 Ga rocks, which is also consistent with the interpretation of *Vendotaenia* as a green or red alga.

Unnamed species

Figure 5

Materials.—Ninety specimens from the Dolores Creek Formation, Mackenzie Mountains Supergroup, near the headwaters of Hematite Creek, Wernecke Mountains, Yukon Territory, Canada; Tonian.

Occurrence.—Dolores Creek Formation, Mackenzie Mountains Supergroup, near the headwaters of Hematite Creek, Wernecke Mountains, Yukon Territory, Canada; Tonian (Maloney et al., 2021).

Description.—Ninety specimens of thin filamentous forms with widths ranging from 30 to 50 μm (Fig. 5) and preserved lengths ranging from 230 to 4,900 μm . Some of these specimens show asymmetrical branching (Fig. 5.1, 5.3, 5.7, 5.9), with a single specimen showing presumed dichotomous branching (Fig. 5.6). These specimens are found on the same bedding planes as *Archaeochaeta guncho* n. gen. n. sp. and were first reported as “smaller Dolores Creek macroalgae” by Maloney et al. (2021).

Remarks.—Simple ribbons can resemble trace fossils in the field. However, there are sharp terminations at the ends of the specimens that would not be expected in trace fossils and instead are likely a result of fragmentation during transport. Cross-cutting relationships are common in trace fossils and not observed in these specimens. Most specimens show minimal distortion of their overall shape, suggesting that the filaments had a degree of structural integrity. A subset of specimens, however, are deformed into J- and C-shaped curves, suggesting these organisms were deformed plastically during transport and burial. This evidence, along with their consistent size, provides support for the biogenicity of the specimens.

The phylogenetic affinity of these specimens remains unresolved due to a lack of morphologically diagnostic characters. The Dolores Creek specimens are poorly preserved and extensively pyritized, which is known to limit the morphological detail in organisms lacking hard parts (Briggs et al., 1996; Petrovich, 2001; Schiffbauer et al., 2014). These fossils contain very limited organic carbon and cannot be extracted by acid dissolution. Continued investigations may help resolve their affinity, but until more diagnostic specimens are recovered, we adopt a conservative approach in their taxonomic treatment.

The size and general morphology of these organisms are similar to the green algal fossil *Proterocladus* Butterfield in Butterfield et al., 1994 reported from Svalbard and North China (Tang et al., 2020). These organisms also resemble extant and

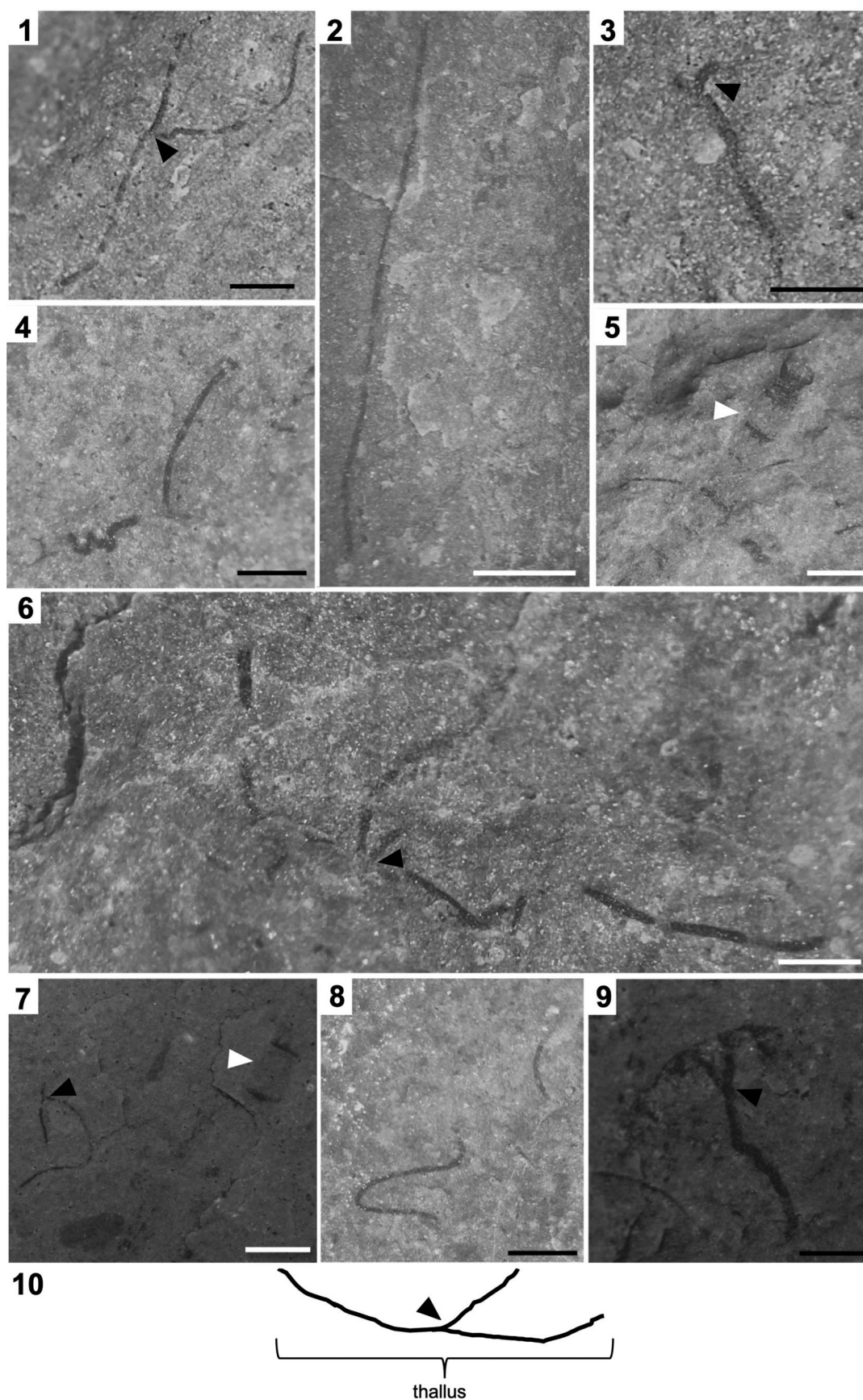


Figure 5. Unnamed Dolores Creek macrofossils. (1, 3, 6, 7, 9) Examples of true branching (black arrows). (2, 4, 5, 8) Examples of non-branching thalli. (5, 7) Smaller macrofossil adjacent to *Archaeochaeta guncho* n. gen. n. sp. (white arrows) to demonstrate size difference between the two taxa. (10) Idealized sketch showing morphological traits. (2, 5–7) White scale bars = 1 mm; (1, 3, 4, 8, 9) black scale bars = 0.5 mm. All specimens from slab ROMIP66167.

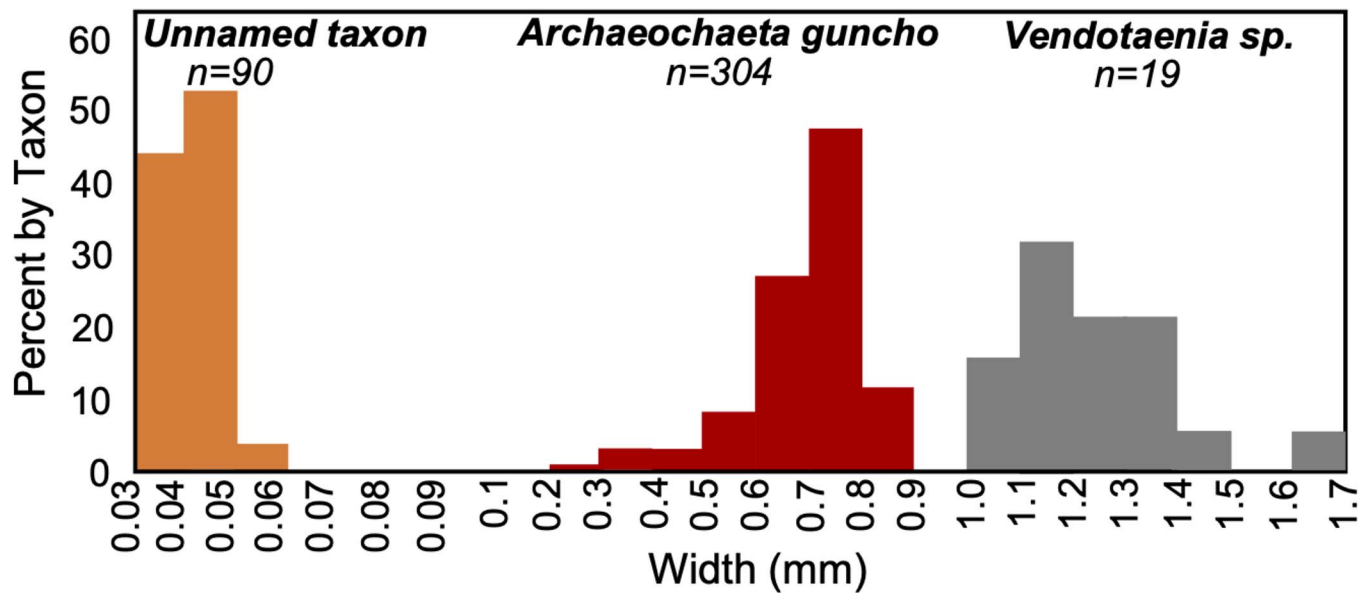


Figure 6. Frequency distribution of fossil width measurements by taxon, showing three separate size classes: the smallest size class ranges from 0.03 to 0.06 mm (unnamed taxon), the medium size class ranges from 0.20 to 0.85 mm (*Archaeochaeta guncho* n. gen. n. sp.), and the large size class ranges from 1.0 to 1.7 mm (*Vendotaenia* sp.). Note the scale on the x axis is different for the unnamed taxon compared with the two other size classes.

fossil false-branching cyanobacteria, such as *Ramivaginalis* Nyberg and Schopf, 1984, *Pseudodendron* Butterfield in Butterfield et al., 1994, “unnamed form 2” in Vorob’eva et al. (2015), and “dichotomously branching filamentous form” in Nagovitsin et al. (2015). *Ramivaginalis* is morphologically similar to the smaller Dolores Creek macrofossils with a branching nonseptate structure (Nyberg and Schopf, 1984). However, the Dolores Creek form taxon is an order of magnitude larger (widths of 30–50 μm versus 4–9 μm ; Sergeev et al., 2012). *Pseudodendron* is another filamentous, branching fossil that is similar in size to the unnamed Dolores Creek specimens, but it is characterized by longitudinal striations, and its branch junctions are reinforced by sheaths (Butterfield et al., 1994; Nagovitsin et al., 2015). *Pseudodendron* is an interesting comparison because it has been interpreted as multiseriate and false branching, similar to modern *Schizothrix*-type cyanobacteria. Nevertheless, the poor preservation of the Dolores Creek forms precludes conclusive assignment to this genus. Unnamed form 2 from the ca. 1500 Ma Kotuikan Formation of Siberia (Vorob’eva et al., 2015) is a dichotomously branching thallus that contains numerous vesicles. It is similar in size to the Dolores Creek form taxon ($\sim 20 \mu\text{m}$ in diameter) but can be distinguished by the spherical vesicles within its branching tubular thallus (Vorob’eva et al., 2015). In addition, unnamed branching fossils from the Tonian Kulady and Khastakh formations in Siberia (Nagovitsin et al., 2015, figs. 9Q–R) resemble the Dolores Creek unnamed filaments. These fossils can be differentiated on the basis of the typical dichotomous branching in the unnamed branching fossils that is exceedingly rare (if even real) in the unnamed species presented here.

Discussion

Detailed investigation of the macrofossil assemblage from the basal Mackenzie Mountains Supergroup reveals at least three distinct organisms. These fossils, along with green algal fossils

from North China (Tang et al., 2020) and probable green algae from the Congo Basin (Sforna et al., 2022), suggest that green algae had colonized marine environments by the early Tonian and likely had profound impacts on their ancient environments by reorganizing seafloor habitats and influencing biogeochemical cycles. Macroalgae utilize bio-essential trace elements, including nitrogen, phosphorus, and metals (e.g., iron and zinc) that are understood to play an important role in the evolution of early life on Earth (Anbar and Knoll, 2002; Erwin et al., 2011; Knoll and Nowak, 2017; Isson et al., 2018). These organisms were also photosynthetic, producing oxygen in shallow marine environments and possibly creating oxygen oases in an ocean with anoxic deep waters (Lyons et al., 2021; H. Wang et al., 2021; Wang et al., 2022).

Interpreting Proterozoic algae.—Early algal fossils remain poorly documented and are fraught by uncertainty. Fossilization of cellular-level tissues can occur only under exceptional taphonomic circumstances. Microfossils and simple macrofossils were understood to dominate the early Neoproterozoic (Xiao and Dong, 2006; Xiao and Tang, 2018) until more recent discoveries of relatively complex macroalgae (Tang et al., 2020; Maloney et al., 2021). These fossils have challenged our understanding of algal ecosystems (e.g., Brocks et al., 2017) and can help calibrate molecular clocks of algal evolution (e.g., Hou et al., 2022).

Enigmatic, long-ranging macroscopic fossils—such as *Chuarina* Walcott, 1899 and *Grypania* Walcott, 1899, both dating back to the Paleoproterozoic (2500–1600 Ma; Hofmann and Jinbiao, 1981; Han and Runnegar, 1992; Schneider et al., 2002), as well as Neoproterozoic vendotaenids (Gnilovskaya, 1971, 1990; Hofmann and Rainbird, 1994; Cohen et al., 2009; Ye et al., 2015)—have also been interpreted as algae (Walter et al., 1976; Vidal, 1989). However, given their simple morphologies and taphonomic limitations, these interpretations have

been questioned (Sun, 1987; Steiner, 1996; Sharma and Shukla, 2009). The ca. 1560 Ma Gaoyuzhuang biota of North China includes large carbonaceous compressions that have also been interpreted as algae (Zhu et al., 2016), but in the absence of cellular preservation or other morphologically informative characters, their phylogenetic placement within broader algae remains uncertain.

There are several other Proterozoic fossils whose algal affinities remain unresolved that are superficially similar to *Archaeochaeta*, including the submillimeter eosolenid tubular fossils from late Mesoproterozoic strata in Siberia (German and Podkovyrov, 2009) and early Neoproterozoic strata in North China (Li et al., 2020). *Proteroarenicola* Wang, 1982, *Pararenicola* Wang, 1982, *Sinosabellidites* Zheng, 1980, and *Parmia* Gnilovskaya et al., 2000 are annulated tubular fossils reported from early Neoproterozoic strata in India (Sharma and Shukla, 2012), North China (Dong et al., 2008; Li et al., 2020), and Russia (Gnilovskaya, 1998). These organisms were first interpreted as worm-like metazoans (Sun et al., 1986) but have been reinterpreted as cyanobacteria (Sharma and Shukla, 2012) or macroalgae (Dong et al., 2008) according to whether the “proboscis-like” structure of Sun et al. (1986) is interpreted as an akinete-like body (Sharma and Shukla, 2012) or a discoidal holdfast structure (Dong et al., 2008).

Although our interpretations are restricted by taphonomy, there is growing evidence that complex algal ecosystems were present in marine environments by the early Neoproterozoic (Fig. 7). The oldest macroscopic green alga is *Proterocladus* from the ca. 1000 Ma Nanfen Formation in North China (Tang

et al., 2020) and the 790 Ma Svanbergfjellet Formation in Spitsbergen, which was recovered along with *Palaeastrum* Butterfield in Butterfield et al., 1994, a colonial-coenobial multicellular green alga comparable to extant hydrodictycean green algae (Butterfield et al., 1994). Ligand conjugated acids that form complexes by binding with metals, specifically nickel-bound geoporphyrin moieties, have been observed in *Arctacellularia tetragonala* Maithy, 1975 from ca. 1000 Ma strata in the Congo Basin. These porphyrins have been interpreted as derivatives of chlorophyll, which supports an algal affinity for these forms (Sforna et al., 2022). Fossils from the Paleoproterozoic Ruyang Group in North China have also been interpreted as green algae, including the organic-walled microfossils *Dictyosphaera* Xing and Liu, 1973, *Shuiyousphaeridium* Yan and Zhu, 1992, and *Gigantosphaeridium* Agić et al., 2015. *Bangiomorpha pubescens* Butterfield, 2000, recovered from strata in the Bylot basins of northeastern Canada, is the oldest unequivocal red algal fossil (Butterfield, 2000; Knoll et al., 2013; Gibson et al., 2018), although still older microfossils from the ca. 1.6 Ga Tirohan Dolomite in central India have also been interpreted as red algae (Bengtson et al., 2017), while younger spores of possible red algal affinity have been reported from Cryogenian rocks in Mongolia (Cohen et al., 2020). The record of diverse eukaryotic fossils from the Mesoproterozoic–Neoproterozoic transition is rapidly expanding and requires detailed descriptions of fossil morphology to understand their role within evolving ecosystems.

Morphological complexity.—Algal complexity increased throughout the Neoproterozoic in two stepwise transitions: (1)

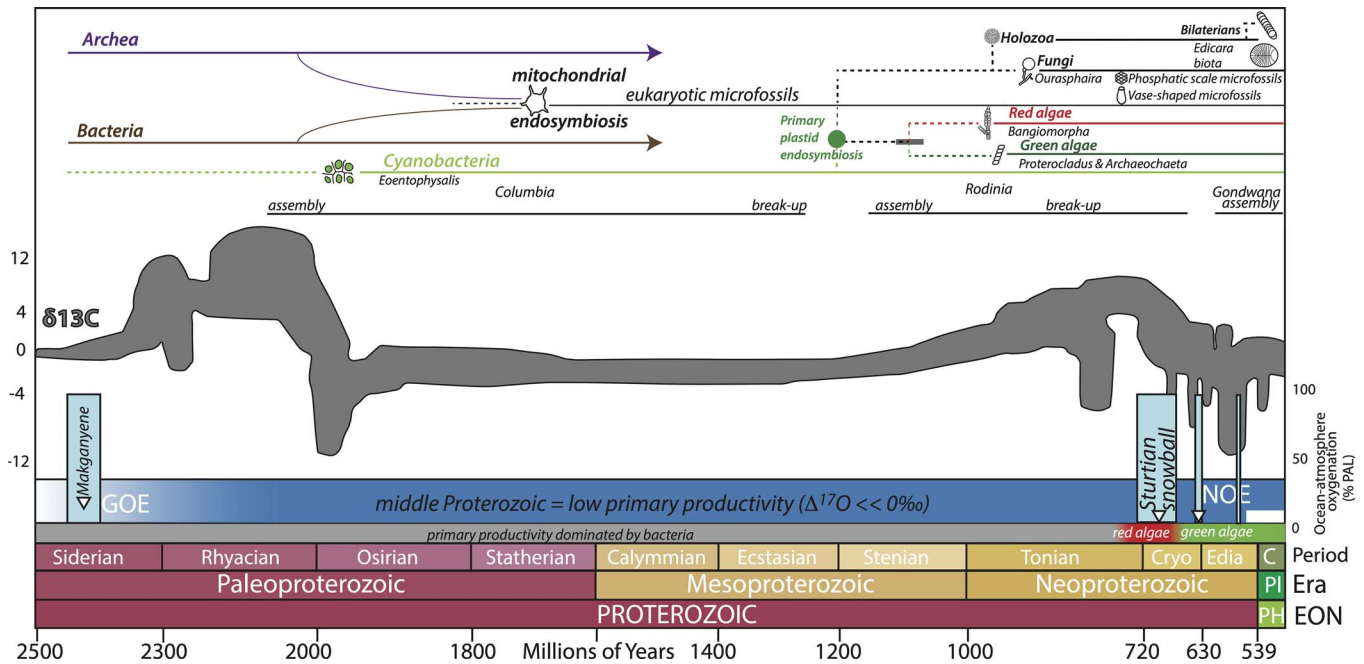


Figure 7. Summary of the evolution and diversification of eukaryotes in the Proterozoic Eon. Examples of documented fossils with age constraints include the cyanobacteria *Eoentophysalis* (Hofmann, 1976; Hodgskiss et al., 2019), fungal microfossils *Oouraspharia* (Loron et al., 2019), red algal microfossils *Bangiomorpha* (Butterfield, 2000; Gibson et al., 2018), green macroalgae *Proterocladus* (Butterfield et al., 1994; Tang et al., 2020), *Archaeochaeta* from the Dolores Creek Formation (this paper), vase-shaped microfossils (Porter and Knoll, 2000; Strauss et al., 2014; Porter and Riedman, 2016; Cohen et al., 2017a), phosphatic microfossils (Cohen and Knoll, 2012; Cohen et al., 2017b), and Ediacaran-type biota (Narbonne and Aitken, 1995; Carbone et al., 2015). Carbon isotopes shown in gray curve from various sources (e.g., Karhu and Holland, 1996; Cox et al., 2016; Hodgskiss et al., 2019); oxygen constraints (Lyons et al., 2014; Sperling et al., 2015), low middle Proterozoic primary productivity (Crockford et al., 2018; Hodgskiss et al., 2020), supercontinent assembly and breakup (Li et al., 2008), and biomarkers (Brocks et al., 2017). Dotted lines are unconstrained. Cryo = Cryogenian Period; Edia = Ediacaran Period; C = Cambrian Period; PI = Paleozoic Era; PH = Phanerozoic Eon.

the emergence of branching macroalgal forms in the early Tonian and (2) a significant increase in maximum size in the Ediacaran (Bykova et al., 2020). The new fossils described here represent important advancements. For example, *Archaeochaeta guncho* and *Vendotaenia* sp. are unusually large for an early Neoproterozoic biosphere typically dominated by organisms represented by microfossils (Cohen and Kodner, 2021). *Vendotaenia* sp. resembles specimens of *Vendotaenia antiqua* from the Nama Group in strata that is almost 400 million years younger. Continued research will provide critical insight into the role of *Vendotaenia* in ancient oceans.

Thallus morphology diversified during the Tonian, as demonstrated by the first examples of dichotomous branching, delicate branching, and putative pseudomonopodial branching (Bykova et al., 2020). Examples include *Longfengshania* Du, 1982 from northwestern Canada (Hofmann, 1985) and the *Sinosabellidites–Protoarenicola–Pararenicola* assemblage from North China (Dong et al., 2008). The unnamed taxon described in the present study has a simple branching pattern (Fig. 5.1, 5.3, 5.7, 5.9), except for one specimen (Fig. 5.6) that suggests relatively more complex branching. However, taphonomic overprinting biases the retention of additional morphological characters necessary for proper phylogenetic assignment. Transport of the fossils by gravity flows aided in their preservation (Maloney et al., 2021) but also contributed to fragmentation of the fossilized specimens, possibly masking more-complex structures and branching. These morphological advancements could indicate ecosystem-level change driven by growing competition for resources and/or space between species (Wang et al., 2015).

The morphological complexity of macroalgal holdfasts also increased throughout the Neoproterozoic, ranging from simple discoidal-globose holdfasts to differentiated rhizomes (Wang et al., 2020; X. Wang et al., 2021). Tonian macroalgae have some of the earliest documented examples of holdfasts, including *Tawuia* Hofmann in Hofmann and Aitken, 1979 (see Xiao and Dong, 2006), *Longfengshania* Du, 1982 (see Hofmann, 1985), and *Protoarenicola* Wang, 1982 (see Du et al., 1986; Dong et al., 2008). Simple discoidal holdfasts are also common in specimens from the Miaohu biota (X. Wang et al., 2021). The holdfasts observed in *Longfengshania* and *Protoarenicola* (Du et al., 1986; Dong et al., 2008) have been described as “deformed globular” because they can be flattened during fossilization (Wang et al., 2020). *Archaeochaeta guncho* have elongated, globose holdfasts best classified as *Gemmaphyton*-type holdfasts (Wang et al., 2020), which are also found in branching algae *Anhuiphyton* Chen et al., 1994 and *Marpolia* Walcott, 1919 from the Ediacaran Lantian biota (X. Wang et al., 2021). To date, holdfasts have not been found in *Vendotaenia* sp., most likely due to their transport as part of density flows, but rounded holdfasts have been reported in *Vendotaenia*-like macroalgae from the Cryogenian Nantuo Formation in South China (Ye et al., 2015). The evolution of holdfasts has been suggested to be driven by transition from stable firm substrates in the Proterozoic to soupy substrates in the Phanerozoic (X. Wang et al., 2021). Simple discs would have been suitable to provide support on a substrate held firm by microbial mats, but a differentiated rhizome holdfast would have been necessary to remain anchored in a soupy substrate. In addition, destabilization of the

substrate may have driven benthic macroalgae to firm, rocky substrates where more complex holdfasts were required (Xiao and Dong, 2006).

Implications for eukaryotic diversity and ecosystems.—The occurrence of centimeter-scale green algae such as *A. guncho* n. gen. n. sp. and *Vendotaenia* sp. in early Tonian strata has implications for the ecological expansion of algae and feedbacks between environmental change and algal diversification. The increase in macroalgal morphological disparity (Bykova et al., 2020), coupled with an increasing diversity of earliest Neoproterozoic macroalgal fossils (Tang et al., 2020), points to an important ecological restructuring of ecosystems by the Tonian Period. Biomarkers from Cryogenian strata suggest that algae overtook cyanobacteria as the dominant primary producers in marine environments after the Sturtian snowball glaciation (Brocks et al., 2017; Brocks, 2018), while other studies report a fundamental shift to eukaryotic-rich ecosystems in the late Tonian (Isson et al., 2018; Zumberge et al., 2020). Although the timings of these studies differ, they concur that ecological restriction of eukaryotes by nutrient limitation is a likely cause for the delayed rise of eukaryotic ecosystems (Brocks et al., 2017; Isson et al., 2018; Zumberge et al., 2020). The hypotheses proposed in these biomarker studies will need to be reconciled with the recent reports of both green macroalgae (Tang et al., 2020; Maloney et al., 2021) and red algal microfossils (Butterfield, 2000; Cohen et al., 2020) during the Mesoproterozoic–Neoproterozoic transition (Cohen and Kodner, 2021). Resolving the taxonomy of Proterozoic macroalgal fossils will aid in understanding and assessing the potential causes of this 300 Myr age gap between the earliest reports of fossil eukaryotic algae (red and green lineages) and their delayed ecological dominance.

Global environmental events have been documented during this transition, including increased oxygenation of the ocean (Planavsky et al., 2015) and biogeochemical cycles (Bykova et al., 2020; Del Cortona et al., 2020), perhaps partially initiated by the emergence of large, photoautotrophic eukaryotes. Their timing suggests a link to the expansion of marine algae and eukaryotic-driven processes, including carbon fixation, filter feeding, and carnivory (Planavsky et al., 2015). These processes influence the habitability of an environment (Sánchez-Baracaldo et al., 2017; Del Cortona et al., 2020) and contribute to establishing oxygenated, nutrient-rich, shallow-marine ecosystems suitable for the emergence of complex animal life and behaviors.

Conclusion

Algae are eukaryotic primary producers that reorganized sea-floor habits and biogeochemical cycles during the Neoproterozoic. Unfortunately, algal fossils are rarely recovered with enough morphological characteristics to establish formal systematic paleontology. Three unique size classes of Tonian fossils are reported from the 950–900 Ma Dolores Creek Formation in the Wernecke Mountains of Northwestern Canada. These are described as *Vendotaenia* sp., *Archaeochaeta guncho*,

and an unnamed taxon. *A. guncho* is interpreted as a benthic green alga, adding to the fossil record of early Tonian chlorophytes. In addition, we consider the current interpretations of vendotaenids as probable green algae on the basis of their large size, limited preservation of holdfasts, and alignment with molecular clocks. The occurrence of benthic macroalgae in the same horizons as two likely photoautotrophs supports the proposal that algae were already playing an important ecological role in ecosystems by the early Tonian. The exceptionally preserved macroalgal fossil assemblage in the Mackenzie Mountains Supergroup provides key insights into increasing ecosystem complexity and influence of algae during the Tonian Period.

Acknowledgments

We are grateful to the First Nation of Na-Cho Nyak Dun for permitting us to conduct fieldwork on their traditional territory. We thank J. Johnny and C. Fraser for their guidance in naming *Archaeochaeta guncho*. This research was supported by a National Science and Engineering Research Council of Canada (NSERC) postgraduate scholarship, Queen Elizabeth II Graduate Scholarship in Science & Technology (QEII-GSST), Geological Society of America Graduate Research Grant, Northern Scientific Training Program, and a Chemical and Physical Sciences Research Visit Program (University of Toronto Mississauga) to K.M.M.; NSERC Undergraduate Student Research Award to D.P.M.; National Science Foundation (NSF) IF 1636643 and NSF CAREER 1652351 to J.D.S.; NSERC Discovery (RGPIN2017-04025), an Agouron Grant, and logistical support from the Polar Continental Shelf Program to G.P.H.; a NASA exobiology Grant (80NSSC18K1086) to S.X.; a NSERC Discovery Grant (RGPIN435402) to M.L.

Declaration of competing interests

The authors declare none.

Data availability statement

Data available from the Dryad Digital Repository: <https://doi.org/10.5061/dryad.hx3ffbjg9>.

References

- Adl, S.M. et al., 2005, The new higher level classification of eukaryotes with emphasis on the taxonomy of protists: *Journal of Eukaryotic Microbiology*, v. 52, p. 399–451.
- Agić, H., Moczyłowska, M., and Yin, L.M., 2015, Affinity, life cycle, and intracellular complexity of organic-walled microfossils from the Mesoproterozoic of Shanxi, China: *Journal of Paleontology*, v. 89, p. 28–50.
- Anbar, A.D., and Knoll, A.H., 2002, Proterozoic ocean chemistry and evolution: a bioinorganic bridge? *Science*, v. 297, p. 1137–1142.
- Barsanti, L., and Gualtieri, P., 2014, *Algae Anatomy, Biochemistry, and Biotechnology*: Boca Raton, Florida, CRC Press, 361 p.
- Becker-Kerber, B. et al. 2021, Clay templates in Ediacaran vendotaeniaceans: implications for the taphonomy of carbonaceous fossils: *GSA Bulletin*, v. 134, p. 1334–1346.
- Bengtson, S., Sallstedt, T., Belivanova, V., and Whitehouse, M., 2017, Three-dimensional preservation of cellular and subcellular structures suggests 1.6 billion-year-old crown-group red algae: *PLoS Biology*, v. 15, n. e2000735, <https://doi.org/10.1371/journal.pbio.2000735>.
- Billy, E., and Wheeler, G., 1998, Northern Tutchone Language Lessons: Carmacks Dialect: Whitehorse, Canada, Yukon Native Language Centre, 1,751 p.
- Briggs, D.E.G., Raiswell, R., Bottrell, S.H., Hatfield, D., and Bartels, C., 1996, Controls on the pyritization of exceptionally preserved fossils: an analysis of the Lower Devonian Hunsrück Slate of Germany: *American Journal of Science*, v. 296, p. 633–663.
- Bringloe, T.T. et al., 2020, Phylogeny and evolution of the brown algae: *Critical Reviews in Plant Sciences*, v. 39, p. 281–321.
- Brooks, J.J., 2018, The transition from a cyanobacterial to algal world and the emergence of animals: *Emerging Topics in Life Sciences*, v. 2, p. 181–190.
- Brooks, J.J., Jarrett, A.J.M., Sirantoine, E., Hallmann, C., Hoshino, Y., and Liyanage, T., 2017, The rise of algae in Cryogenian oceans and the emergence of animals: *Nature*, v. 548, p. 578–581.
- Butterfield, N.J., 1990, Organic preservation of non-mineralizing organisms and the taphonomy of the Burgess Shale: *Paleobiology*, v. 16, p. 272–286.
- Butterfield, N.J., 2000, *Bangiomorpha pubescens* n. gen., n. sp.: implications for the evolution of sex, multicellularity, and the Mesoproterozoic/Neoproterozoic radiation of eukaryotes: *Paleobiology*, v. 26, p. 386–404.
- Butterfield, N.J., 2005a, Reconstructing a complex early Neoproterozoic eukaryote, Wynniatt Formation, Arctic Canada: Lethaia, v. 38, p. 155–169.
- Butterfield, N.J., 2005b, Probable Proterozoic fungi: *Paleobiology*, v. 55, p. 831–856.
- Butterfield, N.J., Knoll, A.H., and Swett, K., 1994, Paleobiology of the Neoproterozoic Svanbergfjellet Formation, Spitsbergen: *Fossils & Strata*, v. 34, 84 p.
- Bykova, N., LoDuca, S.T., Ye, Q., Marusin, V., Grazhdankin, D., and Xiao, S., 2020, Seaweeds through time: morphological and ecological analysis of Proterozoic and early Paleozoic benthic macroalgae: *Precambrian Research*, v. 350, n. 105875, <https://doi.org/10.1016/j.precamres.2020.105875>.
- Cai, Y., Schiffbauer, J.D., Hua, H., and Xiao, S., 2012, Preservation modes in the Ediacaran Gaojiashan Lagerstätte: pyritization, aluminosilicification, and carbonaceous compression: *Palaeogeography, Palaeoclimatology, Palaeoecology*, v. 326–328, p. 109–117.
- Calvo-Pérez, E.A., Molinari-Novoa, E.A., and Guiry, M.D., 2016, Validation of Nostoc flagelliforme (Nostocaceae, Cyanobacteria): *Notulae Algarum*, v. 2, p. 1–2.
- Carbone, C.A., Narbonne, G.M., MacDonald, F.A., and Boag, T.H., 2015, New Ediacaran fossils from the uppermost Blueflower Formation, northwest Canada: disentangling biostratigraphy and paleoecology: *Journal of Paleontology*, v. 89, p. 281–291.
- Cavalier-Smith, T., 1981, Eukaryote kingdoms: seven or nine?: *BioSystems*, v. 14, p. 461–481.
- Chen, M., Xiao, Z., and Yuan, X., 1994, 晚震旦世的特种生物群落——庙河生物群新知 [A new assemblage of megafossils—Miaohé biota from Upper Sinian Doushantuo Formation in eastern Yangtze Gorges, China]: *Acta Palaeontologica Sinica*, v. 33, p. 391–403. [in Chinese]
- Cohen, P.A., and Knoll, A.H., 2012, Scale microfossils from the mid-Neoproterozoic Fifteenmile Group, Yukon Territory: *Journal of Paleontology*, v. 86, p. 775–800.
- Cohen, P.A., and Kodner, R.B., 2021, The earliest history of eukaryotic life: uncovering an evolutionary story through the integration of biological and geological data: *Trends in Ecology & Evolution*, v. 37, p. 246–256.
- Cohen, P.A., and Macdonald, F.A., 2015, The Proterozoic record of eukaryotes: *Paleobiology*, v. 41, p. 610–632.
- Cohen, P.A. et al., 2009, Tubular compression fossils from the Ediacaran Nama Group, Namibia: *Journal of Paleontology*, v. 83, p. 110–122.
- Cohen, P.A., Irvine, S.W., and Strauss, J.V., 2017a, Vase-shaped microfossils from the Tonian Callison Lake Formation of Yukon, Canada: taxonomy, taphonomy and stratigraphic palaeobiology: *Palaeontology*, v. 60, p. 683–701.
- Cohen, P.A., Strauss, J.V., Rooney, A.D., Sharma, M., and Tosca, N., 2017b, Controlled hydroxyapatite biomineralization in an ~810 million-year-old unicellular eukaryote: *Science Advances*, v. 3, n. e1700095, <https://doi.org/10.1126/sciadv.1700095>.
- Cohen, P.A., Vizcaíno, M.N., and Anderson, R.P., 2020, Oldest fossil ciliates from the Cryogenian glacial interlude reinterpreted as possible red algal spores: *Palaeontology*, v. 36, p. 941–950.
- Cox, G.M., Halverson, G.P., Stevenson, R.K., Vokaty, M., Poirier, A.A., Kunzmann, M., Li, Z.X., Denysyn, S.W., Strauss, J.V., and Macdonald, F.A., 2016, Continental flood basalt weathering as a trigger for Neoproterozoic Snowball Earth: *Earth and Planetary Science Letters*, v. 446, p. 89–99.
- Crockford, P.W., Hayles, J.A., Bao, H., Planavsky, N.J., Bekker, A., Fralick, P.W., Halverson, G.P., Bui, T.H., Peng, Y., and Wing, B.A., 2018, Triple oxygen isotope evidence for limited mid-Proterozoic primary productivity: *Nature*, v. 559, p. 613–616.
- Del Cortona, A. et al., 2020, Neoproterozoic origin and multiple transitions to macroscopic growth in green seaweeds: *Proceedings of the National Academy of Sciences of the United States of America*, v. 117, p. 2251–2559.

- Dong, L., Xiao, S., Shen, B., Yuan, X., Yan, X., and Peng, Y., 2008, Restudy of the worm-like carbonaceous compression fossils *Protoarenicola*, *Pararenicola*, and *Sinosabellidites* from early Neoproterozoic successions in North China: *Palaeogeography, Palaeoclimatology, Palaeoecology*, v. 258, p. 138–161.
- Du, R., 1982, The discovery of the fossils such as *Chuarina* in the Qingbaikou System in northwestern Hebei and their significance: *Geology Review* (Beijing), v. 28, p. 1–7.
- Du, R., Tian, L., and Li, H., 1986, Discovery of megafossils in the Gaoyuzhuang Formation of the Changchengian System, Jixian: *Acta Geologica Sinica*, v. 60, p. 115–120.
- Duby, J.E., 1830, *Botanicon Gallicum seu Synopsis Plantarum in Flora Gallica Descripturum. Part 2. Plantas Cellulares Continens* (second edition): Paris, Desray, 601 p.
- Eme, L., Sharpe, S.C., Brown, M.W., and Roger, A.J., 2014, On the age of eukaryotes: evaluating evidence from fossils and molecular clocks: *Cold Spring Harbor Perspectives in Biology*, v. 6, n. a016139, <https://doi.org/10.1101/cshperspect.a016139>.
- Erwin, D.H., Laffamme, M., Tweedt, S.M., Sperling, E.A., Pisani, D., and Peterson, K.J., 2011, The Cambrian conundrum: early divergence and later ecological success in the early history of animals: *Science*, v. 334, p. 1091–1097.
- Gao, K., 1998, Chinese studies on the edible blue-green alga, *Nostoc flagelliforme*: a review: *Journal of Applied Phycology*, v. 10, p. 37–49.
- Gaucher, C., Boggiani, P.C., Sprechmann, P., Sial, A.N., and Fairchild, T., 2003, Integrated correlation of the Vendian to Cambrian Arroyo del Soldado and Corumbá Groups (Uruguay and Brazil): palaeogeographic, palaeoclimatic and palaeobiologic implications: *Precambrian Research*, v. 120, p. 241–278.
- Gaucher, C., Blanco, G., Chigolino, L., Poiré, D., and Germs, G.J.B., 2008, Acratachs of Las Ventanas Formation (Ediacaran, Uruguay): implications for the timing of coeval rifting and glacial events in western Gondwana: *Gondwana Research*, v. 13, p. 488–501.
- German, T.N., and Podkovyrov, V.N., 2009, New insights into the nature of the Late Riphean Eosolenides: *Precambrian Research*, v. 173, p. 154–162.
- Germs, G.J.B., Knoll, A.H., and Vidal, G., 1986, Latest Proterozoic microfossils from the Nama Group, Namibia (South West Africa): *Precambrian Research*, v. 32, p. 45–62.
- Gibson, T.M. et al., 2018, Precise age of *Bangiomorpha pubescens* dates the origin of eukaryotic photosynthesis: *Geology*, v. 46, p. 135–138.
- Gibson, T.M. et al., 2019, Tectono-stratigraphy and facies architecture of the Tonian Hematite Creek and Katherine groups, Wernecke Mountains, Yukon.: Geological Association of Canada/Mineralogical Association of Canada Annual Meeting, v. 42, p. 95.
- Gnilovskaya, M.B., 1971, The oldest aquatic plants of the Vendian of the Russian Platform (late Precambrian): *Paleontological Journal*, v. 5, p. 372–3782.
- Gnilovskaya, M.B., 1983, Vendotaenides, in Urbanek, A., and Rozanov, A.Y., eds., *Upper Precambrian and Cambrian Paleontology of the East European Platform*: Warsaw, Publishing House Wydawnictwa Geologiczne, p. 46–56.
- Gnilovskaya, M.B., 1990, Vendotaenides; Vendian metaphytes, in Sokolov, B.S., and Iwanowski, A.B., eds., *The Vendian System: Volume 1 Paleontology*: New York, Springer-Verlag, p. 138–147.
- Gnilovskaya, M.B., 1998, The ancient annelidomorphs from the upper Riphean of Timan: *Doklady Akademii Nauk*, v. 359, p. 369–372.
- Gnilovskaya, M.B., Veis, A.F., Bekker, A.Y., Olovyanishnikov, V.G., and Raaben, M.E., 2000, Pre-Ediacaran fauna from Timan (annelidomorphs of the late Riphean): *Stratigraphy and Geological Correlation*, v. 8, p. 327–352.
- Gontcharov, A.A., and Watanabe, M., 1999, *Brachythecha sulcata* gen. et sp. nov. (Desmidiaceae, Chlorophyta), a new alga from the highlands of Papua New Guinea: *Phycologia*, v. 38, p. 345–348.
- Graham, L.E., and Wilcox, L.W., 2000, *Algae: Upper Saddle River, New Jersey*, Prentice Hall, 640 p.
- Halverson, G.P., Macdonald, F.A., Strauss, J.V., Smith, E.F., Cox, G.M., and Hubert-Théou, L., 2012, Updated definition and correlation of the lower Fifteenmile Group in the central and eastern Ogilvie Mountains, in MacFarlane, K.E., and Sack, P.J., eds., *Yukon Exploration and Geology 2011: Yukon Geological Survey Annual Report*, p. 75–90.
- Han, T., and Runnegar, B., 1992, Megascopic eukaryotic algae from the 2.1-billion-year-old Negaunee iron-formation, Michigan: *Science*, v. 257, p. 232–235.
- Hermann, T.N., and Podkovyrov, V.N., 2014, Formation of an unusual form of Riphean Eosolenides: *Paleontological Journal*, v. 48, p. 345–352.
- Hermann, T.N., and Timofeev, B.V., 1985, Eosolenides–Novaya Gruppya Problematicheskikh Organizmov Pozdnego Dokembria [Eosolenides—A New Group of Problematical Organisms from the Upper Precambrian]: Moscow, Nauka Press, p. 9–15.
- Hodgskiss, M.S.W., Crockford, P.W., Peng, Y., Wing, B.A., and Horner, T.J., 2019, A productivity collapse to end Earth's Great Oxidation: *Proceedings of the National Academy of Sciences of the United States of America*, v. 116, p. 17207–17212.
- Hodgskiss, M.S.W., Sansjofre, P., Kunzmann, M., Sperling, E.A., Cole, D.B., Crockford, P.W., Gibson, T.M., and Halverson, G.P., 2020, A high-TOC shale in a low productivity world: the late Mesoproterozoic Arctic Bay Formation, Nunavut: *Earth and Planetary Science Letters*, v. 544, n. 116384, <https://doi.org/10.1016/j.epsl.2020.116384>.
- Hofmann, H.J., 1976, Precambrian microflora, Belcher Islands, Canada: significance and systematics: *Journal of Paleontology*, v. 50, p. 1040–1073.
- Hofmann, H.J., 1985, The mid-Proterozoic Little Dal macrobiota, Mackenzie Mountains, north-west Canada: *Paleontology*, v. 28, p. 331–354.
- Hofmann, H.J., and Aitken, J.D., 1979, Precambrian biota from the Little Dal Group, Mackenzie Mountains, northwestern Canada: *Canadian Journal of Earth Science*, v. 16, p. 150–166.
- Hofmann, H.J., and Jinbiao, C., 1981, Carbonaceous megafossils from the Precambrian (1800 Ma) near Jixian, northern China: *Canadian Journal of Earth Sciences*, v. 18, p. 443–447.
- Hofmann, H.J., and Rainbird, R.H., 1994, Carbonaceous megafossils from the Neoproterozoic Shaler Supergroup of Arctic Canada: *Paleontology*, v. 37, p. 721–731.
- Hou, Z., Ma, X., Shi, X., Li, X., Yang, L., Xiao, S., Leliaert, F., and Zhong, B., 2022, Phylotranscriptomic insights into a Mesoproterozoic–Neoproterozoic origin and early radiation of green seaweeds (Ulvophyceae): *Nature Communications*, v. 13, n. 1610, <https://doi.org/10.1038/s41467-022-29282-9>.
- Isson, T.T. et al., 2018, Tracking the rise of eukaryotes to ecological dominance with zinc isotopes: *Geobiology*, v. 16, p. 341–352.
- Karhu, J.A., and Holland, H.D., 1996, Carbon isotopes and the rise of atmospheric oxygen: *Geology*, v. 24, p. 867–870.
- Knoll, A.H., 2014, Paleobiological perspectives on early eukaryotic evolution: *Cold Spring Harbor Perspectives in Biology*, v. 6, n. a016121, <https://doi.org/10.1101/cshperspect.a016121>.
- Knoll, A.H., and Nowak, M.A., 2017, The timetable of evolution: *Science Advances*, v. 3, n. 1603076, <https://doi.org/10.1126/sciadv.1603076>.
- Knoll, A.H., Wörndle, S., and Kah, L.C., 2013, Covariance of microfossil assemblages and microbialite textures across an upper mesoproterozoic carbonate platform: *Palaeos*, v. 28, p. 453–470.
- Krishnamurthy, V., 1962, The morphology and taxonomy of the genus *Compsopogon* Montagne: *Botanical Journal of the Linnean Society*, v. 58, p. 207–222.
- Kützing, F.T., 1845, *Phycologia Germanica, d.i. Deutschlands Algen in bündigen Beschreibungen. Nebst einer Anleitung zum Untersuchen und Bestimmen dieser Gewächse für Anfänger*: Nordhausen, Zu Finden Bei Wilhelm Köhne., 340 p.
- Lauterborn, R., 1907, A new genus of sulfur bacteria (*Thioploca schmidlei* nov. gen. nov. spec.): *Berichte Der Deutschen Botanischen Gesellschaft*, v. 25, p. 238–242. [in German]
- Li, G., Chen, L., Pang, K., Zhou, G., Han, C., Yang, L., Lv, W., Wu, C., Wang, W., and Yang, F., 2020, An assemblage of macroscopic and diversified carbonaceous compression fossils from the Tonian Shiwangzhuang Formation in western Shandong, North China: *Precambrian Research*, v. 346, n. 105801, <https://doi.org/10.1016/j.precamres.2020.105801>.
- Li, Z.X. et al., 2008, Assembly, configuration, and break-up history of Rodinia: a synthesis: *Precambrian Research*, v. 160, p. 179–210.
- Link, H.F., 1820, *Epistola de algis aquaticis in genera disponendis*, in Von Esenbeck, C.D.N., ed., *Horae Physicae Berolinensis: Bonnae, Adolphi Marcus*, p. 1–8.
- LoDuca, S.T., Bykova, N., Wu, M., Xiao, S., and Zhao, Y., 2017, Seaweed morphology and ecology during the great animal diversification events of the early Paleozoic: a tale of two floras: *Geobiology*, v. 15, p. 588–616.
- Loron, C.C., François, C., Rainbird, R.H., Turner, E.C., Borensztajn, S., and Javaux, E.J., 2019, Early fungi from the Proterozoic era in Arctic Canada: *Nature*, v. 570, p. 232–235.
- Lyons, T.W., Reinhard, C.T., and Planavsky, N.J., 2014, The rise of oxygen in Earth's early ocean and atmosphere: *Nature*, v. 506, p. 307–315.
- Lyons, T.W., Diamond, C.W., Planavsky, N.J., Reinhard, C.T., and Li, C., 2021, Oxygenation, life, and the planetary system during Earth's middle history: an overview: *Astrobiology*, v. 21, p. 906–923.
- Macdonald, F.A., Halverson, G.P., Strauss, J.V., Smith, E.F., Cox, G., Sperling, E.A., and Roots, C.F.C.F., 2012, Early Neoproterozoic basin formation in Yukon, Canada: implications for the make-up and break-up of Rodinia Francis: *Geoscience Canada*, v. 39, p. 7–100.
- Maithy, P.K., 1975, Micro-organisms from the Bushimay System (late Precambrian) of Kanshi, Zaire: *The Palaeobotanist*, v. 22, p. 133–149.
- Maloney, K.M. et al., 2021, New multicellular marine macroalgae from the early Tonian of northwestern Canada: *Geology*, v. 49, p. 743–747.
- Maloney, K.M., Schiffbauer, J.D., Halverson, G.P., Xiao, S., and Laffamme, M., 2022, Preservation of early Tonian macroalgal fossils from the Dolores Creek Formation, Yukon: *Scientific Reports*, v. 12, n. 6222, <https://doi.org/10.1038/s41598-022-10223-x>.

- Medig, K.P.R., Thorkelson, D.J., and Dunlop, R.L., 2010, Proterozoic Pinguicula Group: age, stratigraphic contacts, and correlations, *in* Proceedings, GeoCanada 2010—Working with the Earth: Calgary, Canadian Society of Petroleum Geologists, p. 1–3.
- Medig, K.P.R., Thorkelson, D.J., Turner, E.C., Davis, W.J., Gibson, H.D., and Marshall, D.D., 2012, The Proterozoic Pinguicula Group, Wernecke Mountains, Yukon: a siliciclastic and carbonate slope to basin succession with local and exotic sediment provenance: Yukon Geological Survey, p. 129–150.
- Muscente, A.D. et al., 2017, Exceptionally preserved fossil assemblages through geologic time and space: Gondwana Research, v. 48, p. 164–188.
- Nagovitsin, K.E., Rogov, V.I., Marusin, V.V., Karlova, G.A., Kolesnikov, A.V., Bykova, N.V., and Grazhdankin, D.V., 2015, Revised Neoproterozoic and Terreneuvian stratigraphy of the Lena-Anabar Basin and north-western slope of the Olenek Uplift, Siberian Platform: Precambrian Research, v. 270, p. 226–245.
- Narbonne, G.M., and Aitken, J.D., 1995, Neoproterozoic of the Mackenzie Mountains, northwestern Canada: Precambrian Research, v. 73, p. 101–121.
- Nyberg, A.V., and Schopf, J.W., 1984, Microfossils in stromatolitic cherts from the upper Proterozoic Min'yar Formation, southern Ural Mountains, USSR: Journal of Paleontology, v. 58, p. 738–772.
- Pang, K., Tang, Q., Chen, L., Wan, B., Niu, C., Yuan, X., and Xiao, S., 2018, Nitrogen-fixing heterocystous cyanobacteria in the Tonian Period: Current Biology, v. 28, p. 616–622.e1.
- Petrovich, R., 2001, Mechanisms of fossilization of the soft-bodied and lightly armored faunas of the Burgess Shale and of some other classical localities: American Journal of Science, v. 301, p. 683–726.
- Planavsky, N.J., Tarhan, L.G., Bellefroid, E.J., Evans, D.A.D., Reinhard, C.T., Love, G.D., and Lyons, T.W., 2015, Late Proterozoic transitions in climate, oxygen, and tectonics, and the rise of complex life: The Paleontological Society Papers, v. 21, p. 47–82.
- Porter, S.M., and Knoll, A.H., 2000, Testate amoebae in the Neoproterozoic Era: evidence from vase-shaped microfossils in the Chuar Group, Grand Canyon: Paleobiology, v. 26, p. 360–385.
- Porter, S.M., and Riedman, L.A., 2016, Systematics of organic-walled microfossils from the ca. 780–740 Ma Chuar Group, Grand Canyon, Arizona: Journal of Paleontology, v. 90, p. 815–853.
- Rainbird, R.H., Jefferson, C.W., and Young, G.M., 1996, The early Neoproterozoic sedimentary Succession B of northwestern Laurentia: correlations and paleogeographic significance: Bulletin of the Geological Society of America, v. 108, p. 454–470.
- Reichenbach, H.G.L., 1828, *Conspectus Regni Vegetabilis*: Leipzig, C. Cnobloch, 132 p.
- Ritter, J., 2015, Na-Cho Nyak Dun Northern Tutchone Dictionary. <https://www.nndfn.com/wp-content/uploads/2020/05/NNDFN-Dictionary.pdf> [Jun 2022]
- Sánchez-Baracaldo, P., Raven, J.A., Pisani, D., and Knoll, A.H., 2017, Early photosynthetic eukaryotes inhabited low-salinity habitats: Proceedings of the National Academy of Sciences of the United States of America, v. 114, p. E7737–E7745.
- Schiffbauer, J.D., Xiao, S., Cai, Y., Wallace, A.F., Hua, H., Hunter, J., Xu, H., Peng, Y., and Kaufman, A.J., 2014, A unifying model for Neoproterozoic–Palaeozoic exceptional fossil preservation through pyritization and carbonaceous compression: Nature Communications, v. 5, n. 5754, <https://doi.org/10.1038/ncomms6754>.
- Schneider, C.A., Rasband, W.S., and Eliceiri, K.W., 2012, NIH Image to ImageJ: 25 years of image analysis: Nature Methods, v. 9, p. 671–675.
- Schneider, D.A., Bickford, M.E., Cannon, W.F., Schulz, K.J., and Hamilton, M.A., 2002, Age of volcanic rocks and syndepositional iron formations, Marquette Range Supergroup: implications for the tectonic setting of Paleoproterozoic iron formations of the Lake Superior region: Canadian Journal of Earth Sciences, v. 39, p. 999–1012.
- Sergeev, V.N., Sharma, M., and Shukla, Y., 2012, Proterozoic fossil cyanobacteria: The Palaeobotanist, v. 61, p. 189–358.
- Sforna, M.C. et al., 2022, Intracellular bound chlorophyll residues identify 1 Gyr-old fossils as eukaryotic algae: Nature Communications, v. 13, n. 146, <https://doi.org/10.1038/s41467-021-27810-7>.
- Sharma, M., and Shukla, Y., 2009, Taxonomy and affinity of early Mesoproterozoic megascopic helically coiled and related fossils from the Rohtas Formation, the Vindhyan Supergroup, India: Precambrian Research, v. 173, p. 105–122.
- Sharma, M., and Shukla, Y., 2012, Megascopic carbonaceous compression fossils from the neoproterozoic bhima basin, Karnataka, South India: Geological Society Special Publication, v. 366, p. 277–293.
- Silberfeld, T., Leigh, J.W., Verbruggen, H., Cruaud, C., de Reviers, B., and Rousseau, F., 2010, A multi-locus time-calibrated phylogeny of the brown algae (Heterokonta, Ochrophyta, Phaeophyceae): investigating the evolutionary nature of the “brown algal crown radiation”: Molecular Phylogenetics and Evolution, v. 56, p. 659–674.
- South, G.R., and Whittick, A., 1987, An Introduction to Phycology: Oxford, Blackwell Scientific, 341 p.
- Sperling, E.A., Wolock, C.J., Morgan, A.S., Gill, B.C., Kunzmann, M., Halverson, G.P., Macdonald, F.A., Knoll, A.H., and Johnston, D.T., 2015, Statistical analysis of iron geochemical data suggests limited late Proterozoic oxygenation: Nature, v. 523, p. 451–454.
- Stackhouse, J., 1797, Nereis Britannica; continens species omnes fucorum in insulis britannicis crescentium: descriptione latine et anglico, necnon iconibus ad vivum depictis, Fasc. 2: Bath, S. Hazard, p. 31–70.
- Steiner, M., 1996, Chuarial circularis Walcott 1899—“Megasphaeromorph acritarch” or prokaryotic colony?: Acta Universitatis Carolinae, Geologica, v. 40, p. 645–665.
- Strauss, J.V., Rooney, A.D., MacDonald, F.A., Brandon, A.D., and Knoll, A.H., 2014, 740 Ma vase-shaped microfossils from Yukon, Canada: implications for Neoproterozoic chronology and biostratigraphy: Geology, v. 42, p. 659–662.
- Sun, W., 1987, Palaeontology and biostratigraphy of late Precambrian macroscopic colonial algae: Chuarial Walcott and Tawuia Hofmann: Palaeontographica Abteilung B, v. 203, p. 109–134.
- Sun, W., Wang, G., and Zhou, B., 1986, Macroscopic worm-like body fossils from the upper Precambrian (900–700 Ma), Huainan district, Anhui, China and their stratigraphic and evolutionary significance: Precambrian Research, v. 31, p. 377–403.
- Tang, Q., Pang, K., Yuan, X., and Xiao, S., 2020, A one-billion-year-old multicellular chlorophyte: Nature Ecology and Evolution, v. 4, p. 543–549.
- Turland, N.J. et al., 2018, International Code of Nomenclature for Algae, Fungi, and Plants (Shenzhen Code) Adopted by the Nineteenth International Botanical Congress Shenzhen, China, July 2017. Regnum Vegetabile 159: Glashütten, Koeltz Botanical Books, 254 p.
- Turner, E.C., 2011, Stratigraphy of the Mackenzie Mountains supergroup in the Wernecke Mountains, Yukon. Yukon Exploration and Geology 2010: Yukon Geological Survey, p. 207–231.
- Turner, E.C., 2021, Possible poriferan body fossils in early Neoproterozoic microbial reefs: Nature, v. 596, p. 87–91.
- Vidal, G., 1989, Are late Proterozoic carbonaceous megafossils metaphytic algae or bacteria? Lethaia, v. 22, p. 375–379.
- Vorob'eva, N.G., Sergeev, V.N., and Petrov, P.Y., 2015, Kotuikan Formation assemblage: a diverse organic-walled microbiota in the Mesoproterozoic Anabar succession, northern Siberia: Precambrian Research, v. 256, p. 201–222.
- Walcott, C., 1899, Precambrian fossiliferous formations: Geological Society of America Bulletin, v. 10, p. 199–244.
- Walcott, C.D., 1919, Cambrian geology and paleontology IV: Smithsonian Miscellaneous Collections—Middle Cambrian Algae, v. 5, p. 217–260.
- Walter, M.R., Oehler, J.H., and Oehler, D.Z., 1976, Megascopic algae 1300 million years old from the Belt Supergroup, Montana: a reinterpretation of Walcott's Helminthoidichnites: Journal of Paleontology, v. 50, p. 872–881.
- Wang, C. et al., 2022, Strong evidence for a weakly oxygenated ocean—atmosphere system during the Proterozoic: Proceedings of the National Academy of Sciences of the United States of America, v. 119, n. e2116101119, <https://doi.org/10.1073/pnas.2116101119>.
- Wang, G., 1982, Late Precambrian Annelida and Pogonophora from the Huainan of Anhui Province: Bulletin of the Tianjin Institute of Geological Researches, v. 6, p. 9–22. [in Chinese with English abstract]
- Wang, H., Liu, A., Li, C., Feng, Q., Tang, S., Cheng, M., and Algeo, T.J., 2021, A benthic oxygen oasis in the early Neoproterozoic ocean: Precambrian Research, v. 355, n. 106085, <https://doi.org/10.1016/j.precamres.2020.106085>.
- Wang, X., Wu, M., Wan, B., Niu, C., Zheng, W., Guan, C., Pang, K., Chen, Z., and Yuan, X., 2021, Evolution of holdfast diversity and attachment strategies of Ediacaran benthic macroalgae: Frontiers in Earth Science, v. 9, n. 783427, <https://doi.org/10.3389/feart.2021.783427>.
- Wang, X.-L., and Gu, L.-Y., 1984, Observations, on microscopic structure, and ultrastructure of Nostoc flagelliforme: Acta Botanica Sinica, v. 26, p. 484–488. [in Chinese with English abstract]
- Wang, Y., Du, W., Komiya, T., Wang, X.L., and Wang, Y., 2015, Macroorganism paleoecosystems during the middle-late Ediacaran Period in the Yangtze Block, South China: Paleontological Research, v. 19, p. 237–250.
- Wang, Y., Wang, Y., Tang, F., and Zhao, M., 2020, Ediacaran macroalgal holdfasts and their evolution: a case study from China: Palaeontology, v. 63, p. 821–840.
- Xiao, S., and Dong, L., 2006, On the Morphological and Ecological History of Proterozoic Macroalgae, *in* Xiao, S., and Kaufman, A.J., eds., Neoproterozoic Geobiology and Paleobiology: Dordrecht, Springer, p. 57–83.
- Xiao, S., and Tang, Q., 2018, After the boring billion and before the freezing millions: evolutionary patterns and innovations in the Tonian Period: Emerging Topics in Life Sciences, v. 2, p. 161–171.
- Xing, Y., and Liu, K., 1973, On Sinian microflora in Yenliao region of China and its geological significance: Acta Geologica Sinica, v. 1, p. 1–64.

- Yan, Y., and Zhu, S., 1992, Discovery of acanthomorphic acritarchs from the Baicaoping Formation in Yongji, Shanxi and its geological significance: *Acta Micropalaeontologica Sinica*, v. 9, p. 267–282.
- Yang, E.C., Boo, S.M., Bhattacharya, D., Saunders, G.W., Knoll, A.H., Fredericq, S., Graf, L., and Yoon, H.S., 2016, Divergence time estimates and the evolution of major lineages in the florideophyte red algae: *Scientific Reports*, v. 6, n. 21361, <https://doi.org/10.1038/srep21361>.
- Yankauskas, T.V., Mikhailova, N.S., and Hermann, T.N., 1989, *Mikrofossilii Dokembriya SSSR [Microfossils of the Precambrian of the USSR]*: Leningrad, Nauka, 190 p. [in Russian]
- Ye, Q., Tong, J., Xiao, S., Zhu, S., An, Z., Tian, L., and Hu, J., 2015, The survival of benthic macroscopic phototrophs on a Neoproterozoic snowball Earth: *Geology*, v. 43, p. 507–510.
- Yoon, H.S., Nelson, W., Lindstrom, S.C., Boo, S.M., Poeschel, C., Qiu, H., and Bhattacharya, D., 2016, Rhodophyta, in Archibald, J.M., Simpson, A.G.B., and Slamovits, C.H., eds., *Handbook of the Protists*: Cham, Springer, p. 1–45.
- Zheng, W., 1980, A new occurrence of fossil group of *Chuarina* from the Sinian system in north Anhui and its geological meaning: *Bulletin of the Tianjin Institute of Geological Researches*, v. 1, p. 49–69. [in Chinese with English abstract]
- Zhu, S., Zhu, M., Knoll, A.H., Yin, Z., Zhao, F., Sun, S., Qu, Y., Shi, M., and Liu, H., 2016, Decimetre-scale multicellular eukaryotes from the 1.56-billion-year-old Gaoyuzhuang Formation in North China: *Nature Communications*, v. 7, n. 11500, <https://doi.org/10.1038/ncomms11500>.
- Zumberge, J.A., Rocher, D., Love, G.D., Zumberge, A.J., Rocher, D., Love, G.D., Zumberge, J.A., Rocher, D., and Love, G.D., 2020, Free and kerogen-bound biomarkers from late Tonian sedimentary rocks record abundant eukaryotes in mid-Neoproterozoic marine communities: *Geobiology*, v. 18, p. 326–347.

Accepted: 1 December 2022